AD

FAST FERROELECTRIC SPATIAL LIGHT MODULATORS FOR ADAPTIVE OPTICS APPLICATIONS

Final Technical Report

by

Leonid Beresnev

February 1999

United States Army

EUROPEAN RESEARCH OFFICE OF THE U.S.ARMY

London, England

CONTRACT NUMBER N68171-97-5781

Leonid Beresnev

Approved for Public Release; distribution unlimited

18/09 '97 12:51 ☎071 355 5348 N.R.C.C. LONDON

REPORT DOCUMENTATION PAGE

Form Approved
OMB No. 0704-0188

1. AGENCY USE ONLY (Leave Blank)

2. REPORT DATE
10 February 1999

3. REPORT TYPE AND DATES COVERED
Final report (1 Oct.97 - 31 Jan.99)

4. TITLE AND SUBTITLE
Fast ferroelectric spatial light modulators for adaptive optics applications

5. FUNDING NUMBERS
C N68171-97-M-5781
R&D 8323-EE-01

6. AUTHOR(S)
Beresnev Leonid

7. PERFORMING ORGANIZATION NAME(S) AND ADDRESS(ES)
German Telecom Research Center, Am Kavalleriesand 3,
64276 Darmstadt Germany, Prof.Dr.W.Dultz , tel: 49-6151-832560,

8. PERFORMING ORGANIZATION REPORT NUMBER

9. SPONSORING/MONITORING AGENCY NAME(S) AND ADDRESS(ES)
Army Research Laboratory, Dr. J. Ricklin,
ATTN: AMSRL-IS-EE, 2800 Powder Mill Road, Adelphi, MD 20783, USA
tel: (301)394 2535, fax: (301)394 4797. Email: jricklin@arl.mil

10. SPONSORING/MONITORING AGENCY REPORT NUMBER

11. SUPPLEMENTARY NOTES

12a. DISTRIBUTION/AVAILABILITY STATEMENT

12b. DISTRIBUTION CODE

13. ABSTRACT (Maximum 200 words)
Ferroelectric liquid crystals (FLC'S) possessing the DHF (deformed helix ferroelectric) effect were developed with pitch of helix of the order of 0.2μm and spontaneous polarization of the order of 150nC/cm^2 at room temperature. The tilt angle is variable in range 31-42°. The response time τ is variable in range 0.5-5ms, depending on mixture. The refractive indicies of all developed materials were measured. The electrically and optically addressed spatial light modulators (OASLM) were fabricated utilizing the developed mixtures. Phase modulation was measured for double DHF modulator composed from two crossed DHF layers. The phase modulation depth was calculated for different cases of DHF materials. The strong nonlinear increase of the phase shift was found in dependence on voltage in accordance with calculations. The maximum phase shift agreed with the calculations and was equal 0,75λ (λ=wavelength) for cell thicknesses 16 μm, without remarkable dependence on light polarization. Developed OASLM's based on DHF materials with large tilt angle 40° were investigated for real-time holography applications and showed very high figures of merit of basic parameters: diffraction efficiency, spatial resolution and operation rate. The new chemical structure of the DHF liquid crystal molecules was proposed for phase modulation only. Molecules should have banana shape and possess the perfluorinated fragment apart from chiral and dipole fragments. Proposed substances can have ferroelectric as well as antiferroelectric helical smectic packing. Low viscous nematic liquid crystals with high optical anisotropy above 0.25 were tested for phase modulation. Cell with thickness about 3.5μm provided the phase modulation one wavelength in reflecting mode at frequency upto 60Hz. The operation rate for two-frequency nematic liquid crystal was measured upto 250Hz for phase modulation depth half of wavelength in transmissive mode. The increase of modulation depth to one wavelength is assumed by means of increasing the amplitude of applied voltage or using the reflective geometry of modulator. Multi-pixel device was designed for development of computer controlled fast phase modulator, using the low viscous or two-frequency controlled nematic liquid crystals.

14. SUBJECT ITEMS
Phase modulation, ferroelectric liquid crystals, deformed helix ferroelectric effect, electrically controlled refractive indicies, S-effect, two-frequency nematic liquid crystal

15. NUMBER OF PAGES
28

16. PRICE CODE

17. SECURITY CLASSIFICATION OF REPORT	18. SECURITY CLASSIFICATION OF THIS PAGE	19. SECURITY CLASSIFICATION OF ABSTRACT	20. LIMITATION OF ABSTRACT
unclassified	unclassified	unclassified	

NSN 7540-01-280-5500

Standard Form 298 (Rev. 2-89)
Prescribed by ANSI Std. Z39-18
298-102

ATTACHMENT 1 PAGE 1

Abstract.

Electrically and optically addressed spatial light modulators for gray scale phase modulation are developed with high operation rate. As an electrooptical media the ferroelectric liquid crystal mixtures are developed with response time in range 0.2 - 0.5ms. Developed FLC materials FLC-471, FLC-510, FLC-512 have very large tilt angle 40-42 degrees and very short pitch of helix less than 0.2 mkm. The electrical control of averaged refractive index indicatrix is explored using the DHF (deformed helix ferroelectric) effect. The gray scale phase modulation only is obtained using two DHF modulating layers mounted in series. The calculations of the phase modulation by single and double DHF layer were made using the real parameters of the developed materials. The unipixel prototype of modulator is fabricated and tested in interferometric scheme. The strong nonlinear behaviour of the phase shift versus d.c. electric field was found. The quantitavite results agree with the theoretical calculations.

The new structure of molecules is proposed for synthesis of ferroelectric liquid crystals for phase modulation and detail calculations of the change of refractive indicies in dependence on molecular tilt angle and applied electric field are made.

The optically addressed spatial light modulators (OASLM's) are developed using the DHF materials with very large tilt angle and with operation rate in range of hundreds Hertz. The phase shift between black and illuminated areas reaches 160 degrees. The device shows the record diffraction efficiency for non-polarized read-out light exceeding 20% at spatial resolution 100lp/mm. The operation of device in holographic scheme of correction of telescope aberration in real time is shown. The preliminary experiments were made for holofraphic correction of severe phase distorsion in optical systems.

Nematic liquid crystal mixtures with high refractive index anisotropy Δn=0.27 were tested for phase modulation only using S-effect. The estimated operation rate is about 60 Hz for phase modulation 2π in reflective mode.

One-pixel SLM for phase modulation was fabricated and tested using two frequency addressed nematic liquid crystal ZhKM-1001 having the high refractive index anisotropy Δn = 0.25 and change of sign of dielectric anisotropy $\Delta\varepsilon$ from +2.5 to -2.5 at increase of frequency from 500Hz to 20kHz. The enhanced operation rate exceeding 200Hz was obtained for phase modulation 0-π in transmissive mode. The techniques for preparation of planarly oriented nematic liquid crystals are developed and substrates for multi-pixelized electrically addressed SLM as well as connecting interfaces between SLM and computer are designed.

1. Historical Background.

The problem of wave front control is among the most important for developement of many optical systems [1], e.g. astronomical [2] and ground to ground imaging devices [3], optical communication systems, laser lidars, systems for optical turbulence simulation [4], etc. The wavefront is corrected usually using mechanically controlled mirrors, and electrically or optically controlled refractive index based devices such as photorefractive crystals, liquid crystal modulators (usually LC TV panels) and liquid crystal light valves.. Mechanically controlled mirrors are rather expensive and do not provide required high resolution for wavefront correction.. The use of optical media with controlled refractive index has potentions for fast, high resolution and low costs wavefront control. The main drowbacks of photorefractive materials for wavefront correction applications are the following: slow time response, relatively small change of refractive index and small aperture size.

Liquid crystals as media with electrically controlled optical parameters, e.g. deviation and deformation of local refractive index indicatrix are considered among the most perspective materials for wavefront control. The main electrooptical effects in liquid crystals are accompanied by simultaneous change of both, phase and polarization. The later is undesirable effect if we consider adaptive optics and other applications where phase modulation is required.

Only S-effect in nematic liquid crystals can provide the pure phase change of polarized light with polarization plane along the director of parallel alignment nematic liquid crystal. This parallel aligned nematic is used as pixelized electrically controlled phase modulator [5] as well as optically addressed spatial light modulator (SLM), containing the photoconducting layer [6].

In both cases the operation speed of SLM is restricted by several tens of milliseconds for phase modulation depth in order of 2π. To obtain significant phase change $\Phi > 2\pi$ at common refractive index anisotropy $\Delta n \sim 0.15$, the LC cell thickness d should be of the order of 5µm for wavelength 0.633µm. The relaxation time of nematic liquid crystal strongly depends on cell thickness [7] and in mentioned case will be not less than tens of milliseconds.

It means that resulting operation rate for commonly used nematic LC based wavefront correctors can not exceed several Hz.

Ferroelectric liquid crystals.

Ferroelectric liquid crystals (FLC's) discovered in 1975 [8] allowed us to design the electrooptical devices with much higher operation rate in comparison with nematic liquid crystals. The response time can be in microsecond range [9]. Number of efforts were made last years to realize the attractive properties of FLC's in display and non-display applications [10, 11, 12] The main electroptical property of FLC's, considered so far for applications, is the electrically controlled switching or deviation of optical indicatrix in plane of transparent electrodes. The change of refractive index is considered as very small and change of phase is negligible in FLC cell's with commonly used thickness 1-1.5μm. Only one FLC material demonstrated measurable change of refractive index under applied electric field [13].

Deformed helical ferroelectric effect in chiral smectic C liquid crystals.

We have found in 1987 [14] that in helical chiral smectic C* materials with short pitch of helix of the order of 0.3μm and high value of spontaneous polarization P_s of the order of $100nC/cm^2$ the electric field, applied along smectic layers induces the significant deformation of refractive index indicatrix at relatively small values of applied voltage in range of units Volts. It was found also, that response time doesn't depend on driving voltage and can be of the order of hundreds microseconds [15, 16]. It was shown, that strong change of anisotropy of refractive index of the order of 0.05 between electric field free state $<\Delta n>$ and unwound uniform state Δn takes placee. The change of refractive index of DHF materials was recently tested in such devices as electrically controlled Fabri Perot etalon [17] and phase gratings applied for fast adaptive lens [18].

In case of change of refractive index 0.05 we need relatively thin cell with thickness d of the order of 10-12μm for obtaining the phase shift 2π. Due to independence of electrooptical response time on cell thickness there is the possibility to design the SLM with gray scale phase modulation having low driving voltages of the order of 5-10 V and short response time in sub-millisecond range, that is 2-3 orders faster than operation speed of nematic liquid crystals.

2. Technical Approach.

We have considered the following approaches to develop fast liquid crystal phase modulators.

At first, the deformed helix ferroelectric (DHF) effect was considered as a material with strong dependence of shape and inclination of refractive index indicatrix on applied electric field. To receive the pure phase modulation it was proposed to use two DHF modulators mounted in series. See sections 2.1.2 and 4.1.

At second, the new shape of molecules forming the lamellar smectic phase was proposed for chemical synthesis, to receive the pure phase modulation in one FLC layer only. This approach is described in sections 2.1.3 and 2.1.4.

At third, the FLC materials with very large tilt angle were developed and applied for design of fast optically addressed spatial light modulators. Such devices allowed us to compensate very strong aberrations in optical systems, using the holographic technique. This OASLM and their use in holographic corrector of severe telescope aberration is described in section 5. Preliminary measurements were made for use of these modulators in holographic correctors of severe phase distorsion.

At fourth, we tested the nematic liquid crystals with large anisotropy of refractive index $\Delta n=0.27$ for preparation electrically and optically addressed spatial light modulators with phase control in range $0-2\pi$. High value of Δn allows us to design the liquid crystal layer with small thickness, and hence the relaxation time was reduced to units of millisecond, section 6. We developed also the fast phase modulator using the nematic liquid crystal with the change of sign of dielectric anisotropy $\Delta\varepsilon$ at increase of frequence of applied voltage. It was found the enhanced operation rate with operation rate faster than 200 Hz for electrically addressed phase modulator, section 7. To utilize the both nematic liquid crystals for fabrication of phase modulators the special mosaic multi-pixel architecture is designed to control independently any pixel of mosaic, section 8.

2.1. Calculations of the phase modulation for DHF (deformed helix ferroelectric) liquid crystal layers.

DHF effect proposed by author with co-workers [14] is considered as a most sensitive electroptical effect in liquid crystal and tenths of Volt is enough to induce the significant deviation $<\Theta_o>$ (35 in Fig.1) of optical axis $<n_{\|}>$ (31 in Fig.1) of averaged optical refractive index indicatrix 30, Fig.1. This deviation takes place with considerable change of the values of both components $<n_{\|}>$ (31, Fig.1) and $<n_{\perp}>$ (32, Fig.1).

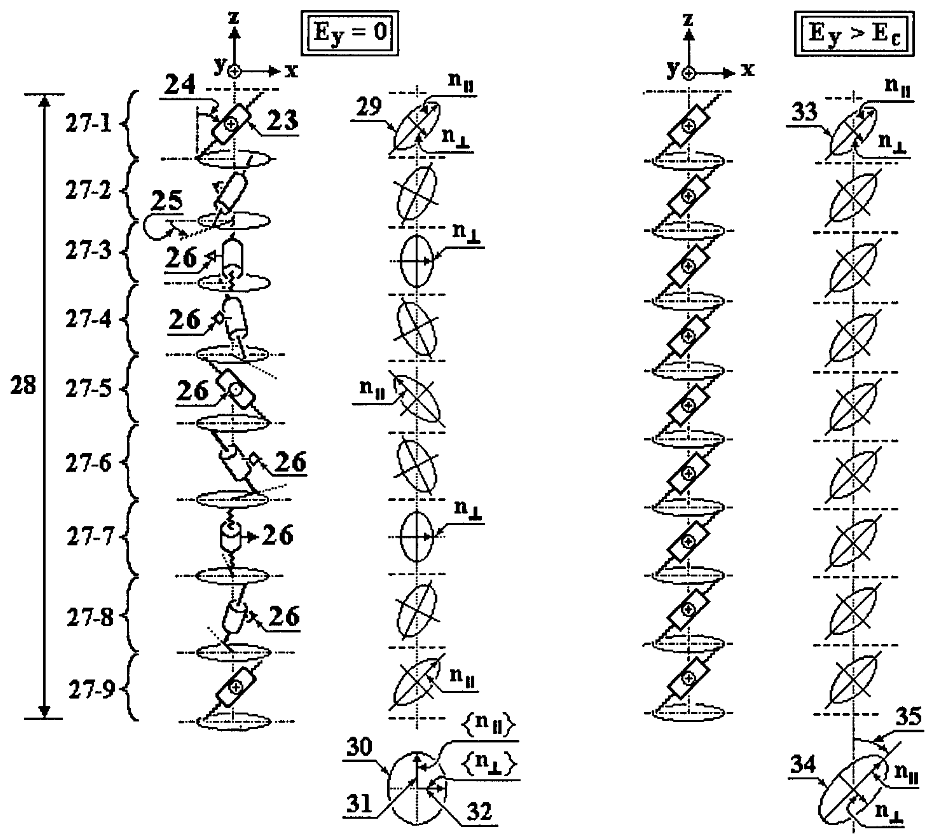

Fig.1. Helical structure of strongly twisted smectic C phase without electric field (left) and under application of the untwisting voltage (right).

2.1.1. *Calculation of the averaged refractive indices of helical FLCs*

Refractive indices are calculated by averaging the elements of the dielectric tensor (for optical frequencies) over a full helical pitch considering all possible orientations of the molecules. The calculations start with a (hypothetic) totally unwound phase with the tensor

$$\boldsymbol{\varepsilon}^{mol} = \begin{bmatrix} \varepsilon_{\perp 1} & 0 & 0 \\ 0 & \varepsilon_{\perp 2} & 0 \\ 0 & 0 & \varepsilon_{\|} \end{bmatrix} = \begin{bmatrix} n_{\perp 1}^2 & 0 & 0 \\ 0 & n_{\perp 2}^2 & 0 \\ 0 & 0 & n_{\|}^2 \end{bmatrix} \tag{1}$$

(in general we should take the biaxiality of the unwound state into account, therefore one must distinguish between two perpendicular indices). The local dielectric tensor for a helical structure can be calculated by simple geometrical transformations described by the angles θ (tilt) and φ, according to the figure 2.

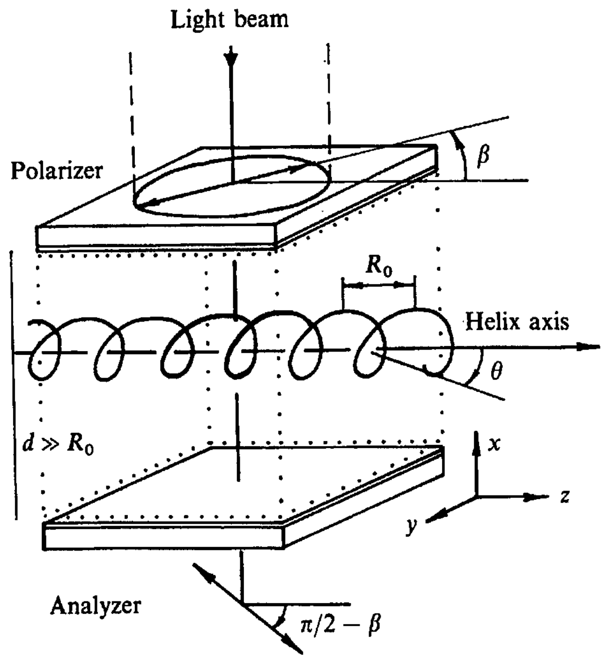

Fig.2. Geometry of observation of DHF effect.

Thus one gets

$$
\begin{aligned}
&\varepsilon_{11}^{loc} = \varepsilon_{\perp 1}\cos^2\theta\cos^2\varphi + \varepsilon_{\perp 2}\sin^2\varphi + \varepsilon_{\parallel}\sin^2\theta\cos^2\varphi \\
&\varepsilon_{12}^{loc} = \left(-\varepsilon_{\perp 1}\cos^2\theta + \varepsilon_{\perp 2} - \varepsilon_{\parallel}\sin^2\theta\right)\sin\varphi\cos\varphi \\
&\varepsilon_{13}^{loc} = -\Delta\varepsilon_1 \sin\theta\cos\theta\cos\varphi \\
&\varepsilon_{21}^{loc} = \varepsilon_{12}^{loc} \\
&\varepsilon_{22}^{loc} = \varepsilon_{\perp 1}\cos^2\theta\sin^2\varphi + \varepsilon_{\perp 2}\cos^2\varphi + \varepsilon_{\parallel}\sin^2\theta\sin^2\varphi \\
&\varepsilon_{23}^{loc} = \Delta\varepsilon_1 \sin\theta\cos\theta\sin\varphi \\
&\varepsilon_{31}^{loc} = \varepsilon_{13}^{loc} \\
&\varepsilon_{32}^{loc} = \varepsilon_{23}^{loc} \\
&\varepsilon_{33}^{loc} = \varepsilon_{\perp 1}\sin^2\theta + \varepsilon_{\parallel}\cos^2\theta
\end{aligned}
\qquad (2)
$$

with $\Delta\varepsilon_1 = \varepsilon_{\parallel} - \varepsilon_{\perp 1}$. For a perfect (undeformed) helix there is an equal distribution of the molecular orientations in respect to the angle φ and one can calculate the average values in dependence on the tilt angle θ:

$$
\begin{aligned}
&\varepsilon_{11}^{helix} = (\varepsilon_{\perp 1}\cos^2\theta + \varepsilon_{\perp 2} + \varepsilon_{\parallel}\sin^2\theta)/2 \\
&\varepsilon_{22}^{helix} = \varepsilon_{11}^{helix} \\
&\varepsilon_{33}^{helix} = \varepsilon_{\perp 1}\sin^2\theta + \varepsilon_{\parallel}\cos^2\theta
\end{aligned}
\qquad (3)
$$

Thus the refractive indices of the helix are given by

$$< n_{\perp} > = \sqrt{\varepsilon_{11}^{helix}} = \sqrt{(\varepsilon_{\perp 1}\cos^2\theta + \varepsilon_{\perp 2} + \varepsilon_{\parallel}\sin^2\theta)/2} = \sqrt{(n_{\perp 1}^2\cos^2\theta + n_{\perp 2}^2 + n_{\parallel}^2\sin^2\theta)/2}$$

$$< n_{\|} >= \sqrt{\varepsilon_{33}^{helix}} = \sqrt{\varepsilon_{\perp 1} \sin^2\theta + \varepsilon_{\|} \cos^2\theta} = \sqrt{n_{\perp 1}^2 \sin^2\theta + n_{\|}^2 \cos^2\theta} \tag{4}$$

From these equations one can calculate the refractive indices of DHF materials in dependence on the tilt angle. The figure 3 shows two examples with different molecular indices as indicated.

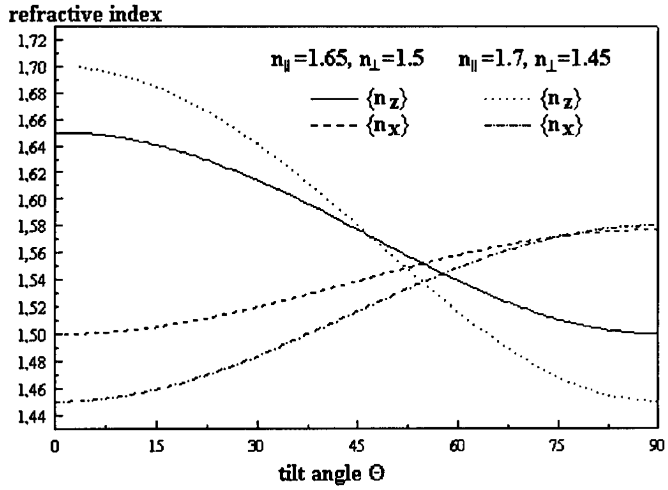

Fig.3. The effective refractive indices of DHF materials in dependence on the tilt angle.

Inversion of equation 4 allows one to calculate the molecular refractive indices of the unwound phase when the averaged values of the helical structure are known by

$$\begin{aligned} n_{\|} &= \sqrt{\frac{2n_{\perp}^2 \sin^2\theta - n_{\|}^2 \cos^2\theta}{\sin^4\theta - \cos^4\theta}} \\ n_{\perp} &= \sqrt{\frac{2n_{\perp}^2 \cos^2\theta - n_{\|}^2 \sin^2\theta}{\cos^4\theta - \sin^4\theta}}, \end{aligned} \tag{4a}$$

where $n_{\|}$ and $n_{\perp}$ are measured values of the averaged indices.

For the calculation of average values of deformed helix structures an additional variation of the angle φ with the coordinate z along the helical axis in dependence on the electrical field E must be considered. In this case average values $< \cos^2\varphi >$ and $< \sin^2\varphi >$ will vary with the value of E as well as $< \sin\varphi >$ (which is zero in the perfect helix). The averages $< \sin\varphi \cos\varphi >$ and $< \cos\varphi >$ will be zero even for the deformed helix. Thus the tensor of the dielectric constant of the DHF material is given by

$$\begin{aligned} \varepsilon_{11}^{DHF} &= (\varepsilon_{\perp 1} \cos^2\theta + \varepsilon_{\|} \sin^2\theta) < \cos^2\varphi > + \varepsilon_{\perp 2} < \sin^2\varphi > \\ \varepsilon_{22}^{DHF} &= (\varepsilon_{\perp 1} \cos^2\theta + \varepsilon_{\|} \sin^2\theta) < \sin^2\varphi > + \varepsilon_{\perp 2} < \cos^2\varphi > \\ \varepsilon_{23}^{DHF} &= \varepsilon_{32}^{DHF} = \Delta\varepsilon_1 \sin\theta \cos\theta < \sin\varphi > \\ \varepsilon_{33}^{DHF} &= \varepsilon_{\perp 1} \sin^2\theta + \varepsilon_{\|} \cos^2\theta \\ \varepsilon_{12}^{DHF} &= \varepsilon_{21}^{DHF} = \varepsilon_{13}^{DHF} = \varepsilon_{31}^{DHF} = 0 \end{aligned} \tag{5}$$

According to Pikin [19] the angle φ can be described in the linear regime by

$$\varphi(z) = q_0 z + \tilde{E} \cos(q_0 z), \tag{6}$$

where $\tilde{E} = E / E_c$ is the electric field E normalized to the critical field E_c for unwinding of the helix. With (6), the average values in (5) can be easily calculated numerically. After the calculation of the averaged dielectric tensor, the tensor matrix is diagonalized. The rotation angle gives the rotation angle of the optical indicatrix and the eigenvalues give the refractive indices squared.

Examples for two sets of molecular indices are shown below (molecular biaxiality is neglected, i. e. $n_{\perp 1} = n_{\perp 2}$).

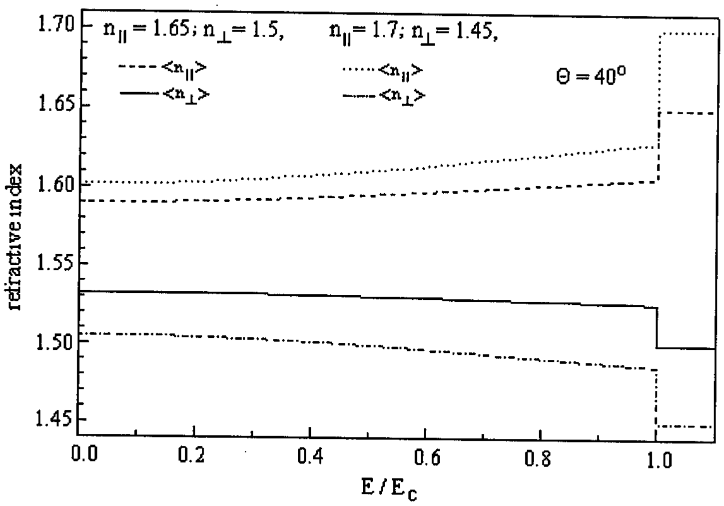

Fig.4. Examples of electric field behaviour of averaged refractive indicies.

The model is only valid in the linear regime, i. e. for values $\tilde{E} = E / E_c < 1$ and doesn't represent the behavior at the critical field value $\tilde{E} = 1$. Nevertheless experiments [17] have shown that the behaviour is very similar as shown in the figure with nearly comparable sharp edge at the critical field (in the figure a jump to the totally unwound state is considered).

The rotation angle doesn't depend on the refractive indices at a fixed tilt angle. For the above presented examples with a tilt angle of Θ=40° the following behaviour can be calculated, Fig.5.

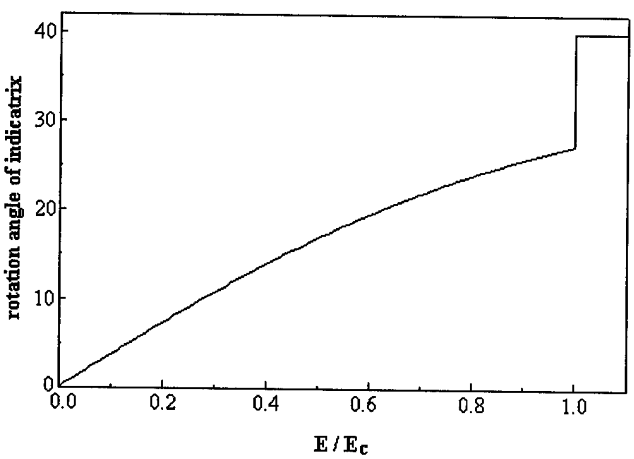

Fig.5. The field dependence of the deviation of averaged refractive index indicatrix.

In contrast to the refractive indices the electrically controllable rotation angle in the linear regime covers a major part of the molecular tilt angle.

The comparison of refractive indices of the helical and the totally unwound structure allows one also to calculate the upper limit for the modulation of the indices by an electric field and also the upper limit for the effective index modulation by crossed DHF cells for any polarization direction.

2.1.2. *Double DHF modulator.*

The deformation of helical structure of DHF material under electric field is accompanied with deviation of refractive index indicatrics and this leads to strong change of light polarization state. This change of polarization induces considerable parasitic influence on light intensity in schemes, containing polarizing elements. To compensate the strong change of light polarization state we supposed to use two identical DHF layers mounted in series. It will be no dependence on the polarization of light beam, if these cells are oriented in such a manner, that slow opical axes <n"> of both DHF layers are perpendicular to each other, Fig.6. This property of two crossed equal uniaxial optical plates doesn't depend on thickness of plates provided that both cells are identical.

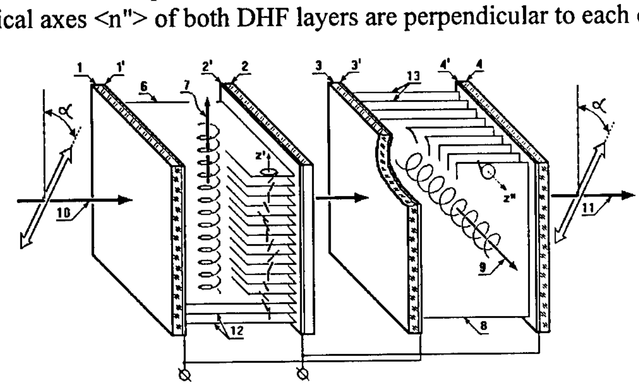

Fig.6. Polarization non-sensitive DHF phase modulator composed from two crossed DHF cells.

It means that we can obtain gray scale phase only modulation if the optical index indicatrices of both DHF layers will be affected, at first, simultaneously in equal manner, and at second, the deviations of optical refractive index ellipsoids should be synchronized to conserve always their perpendicular mutual orientation, Fig.7.

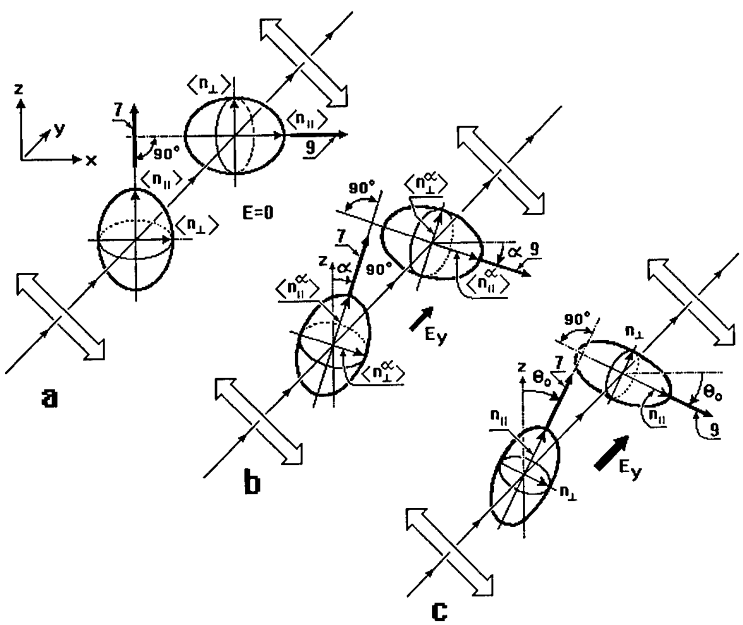

Fig.7. Change of shape and inclination of refractive index ellipsoides in two crossed DHF cells under increase of applied electric field E. The long axes of ellipsoids concerve the mutual perpendicular orientation.

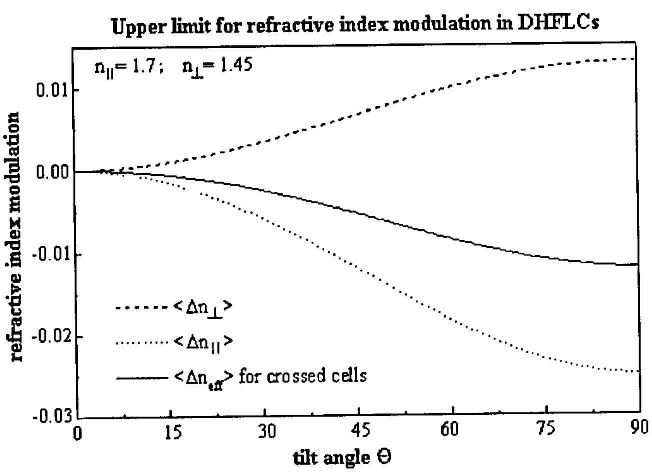

Fig.8. Upper limit for change of refractive index anisotropies for separate DHF cells and for two crossed cells in dependence on molecular tilt angle.

Additional advantage of two crossed DHF cells apart from polarization independence is the significant compensation of wavelength dispersion. It is known for two uniaxial optical plates, mounted in serious [20], and was recently found experimentally for two electroclinic FLC layers [21, 22].

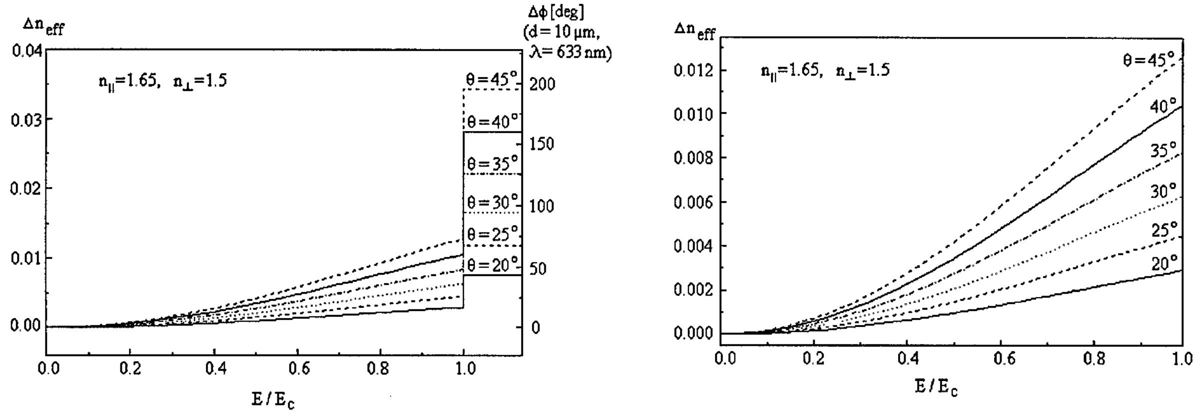

Fig.9. Effective value of refractive index for two crossed DHF cells in dependence on applied electric field E normalized to the untwistingl value E_c. Right picture - after magnification along ordinate. Refractive indices of the the unwound helix are $n_{\|} = 1.65$, $n_{\perp} = 1.5$. The right scale in the left picture presents the calculated phase shift for $\lambda = 633$ nm and for thickness of one cell d = 10 µm. θ is the molecular tilt angle.

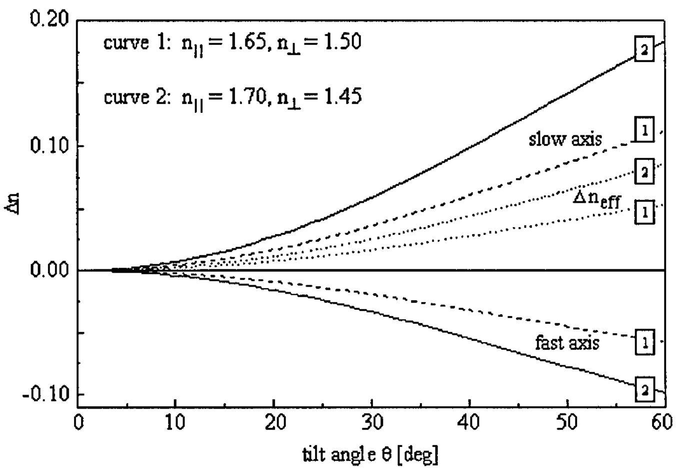

Fig.10. Calculated upper limit of the modulation of the refractive indices in dependence on the molecular tilt angle θ. Δn_{eff} for two crossed DHF cells

The values are calculated as the difference of the refractive indices of the unwound state and the undisturbed helical state. The two upper curves represent the slow optical axis, the two lower curves represent the fast optical axis and the two curves in the middle represent the effective value of the refractive index change of two crossed DHF cells (Δn_{eff}). Numbers 1 and 2 indicate two different sets of refractive indices for the unwound state (curves 1: $n_{\|} = 1.65$ and $n_{\perp} = 1.5$; curves 2: $n_{\|} = 1.7$ and $n_{\perp} = 1.45$.

2.1.3. New approach to the design of liquid crystal material for phase modulation.

DHF materials composed from banana shape molecules.

In frames of this work we have proposed the new molecular structure for liquid crystal, Fig.11, having the electrically controlled change of the refractive index ellipsoid 13, which is not accompanied with the deviation of their long axis 14. The liquid crystal consists of molecules 1, having two electronic polarizable central cores 2 and 3, connected with each other with neutral molecular tales, e.g. alyphatic, siloxane and/or fluorinated chains. Mentioned cores 2 and 3 form the chevron or banana dimer molecule. The cores 2 and 3 do form the angles 4 and 5 with nornal to smectic layers z of the opposite signs. These molecules do form the layer structure, for instance smectic phase with the layers 7, 7-1, 7-2, 7-3 etc.The averaged refractive index ellipsoid 13 of the smectic phase composed from such molecules 1, can be

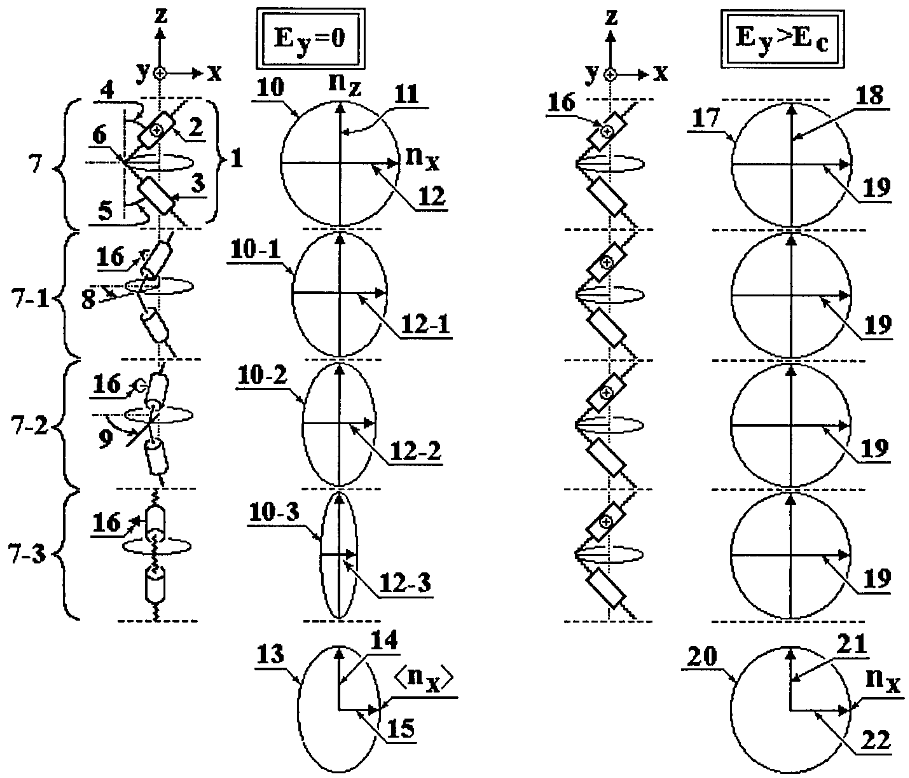

Fig.11. The banana shape structure of the proposed molecules 1, composing the smectic liquid crystal for phase modulation. The averaged refractive index ellipsoid 13 conserves their orientation along the normal z to smectic layers 7, 7-1, 7-2 ... in the helical structure. Under the action of electric field E_y applied along the smectic layers the refractive index $\langle n_x \rangle$ perpendicular to the normal z does change. It is shown the quarter part of the turn of helix.

described by tensor with long axis 14 along the normal z to the smectic layers. For any change of the azimuthes of tips 6 of dimer molecules the projection of the tensor of refractive index 13 (refractive index ellipsoid) will be characterized by elipsoids 10, 10-1, 10-2, 10-3....Long axes 11 of these ellipsoids are always directed along the normal z to smectic layers.

Chevron planes form the helical structure with short helical pitch of the order of or less than wavelength of light, if go along the normal z to smectic layers 7, 7-1, 7-2, 7-3,... In undeformed state, without electric field, the averaged refractive index indicatrix 13 is described by ellipsoid of rotation with the axis 14 of rotation along the normal z to smectic layers. The weak electric field E_y does disturb the helical structure in such a manner that all chevron planes, as well as all tips 6, have the tendency to be oriented in plane perpendicular to the electric field. In cross-section of the averaged refractive index elipsoid the axis 15 along the smectic layer x and perpendicular to the electric field E_y, will be increased, whereas the axis 14 along the normal z to the smectic layers will be unchanged.

The helical structure is related with the chiral fragment introduced into the one or both external tails of the molecules. These fragments induce the spontaneous polarization with local dipole moments 16 of separate molecules along the smectic layers and perpendicular to the molecular chevron plane. Due to interaction of these molecular dipole moments 16 the weak electric field E_y is enable to deform the helical structure up to total unwounding of helix, right part of Fig.11. The averaged refractive index ellipsoid 13 transforms to the molecular one 20 with the component of the refractive index 21 along the normal z to smectic layers and with the value which does not change and is equal to the component 11 of the molecular refractive index 10.

The component 22 of the refractive index ellipsoid 20 transforms from the averaged component 15 to the molecular one 22 with the smooth increase under increase of the value of the electric field E_y. It means that for light polarization along the smectic layer x the phase shift of wavefront will takes place whithout the deviation of the polarization plane. The value of the phase change $\delta\Phi$ is determined with the difference between components 22 and 15, that is $\delta n_x = \langle n_x \rangle - n_x$, and $\delta\Phi = d\,(\langle n_x \rangle - n_x)$, where d is the cell thickness.

The directions of the chevron edges (tips 6) in neighbour smectic layers can have 1) the same or 2) the opposite orientations.

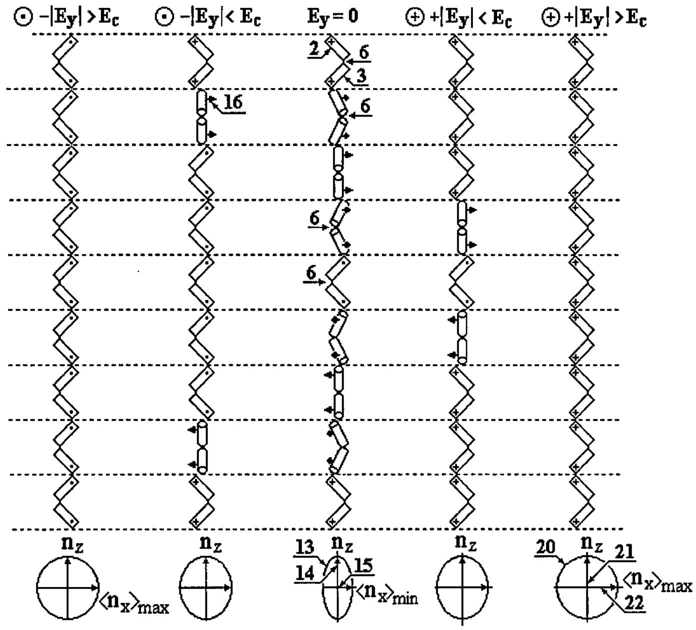

The version 1) corresponds to the ferroelectric molecular packing, as it shown in Fig.12.

Fig.12. Ferroelectric packing of neighbour smectic layers, composed from banana shape molecules.

The version 2) corresponds to the antiferroelectric packing, as it is shown in the following Fig.13.

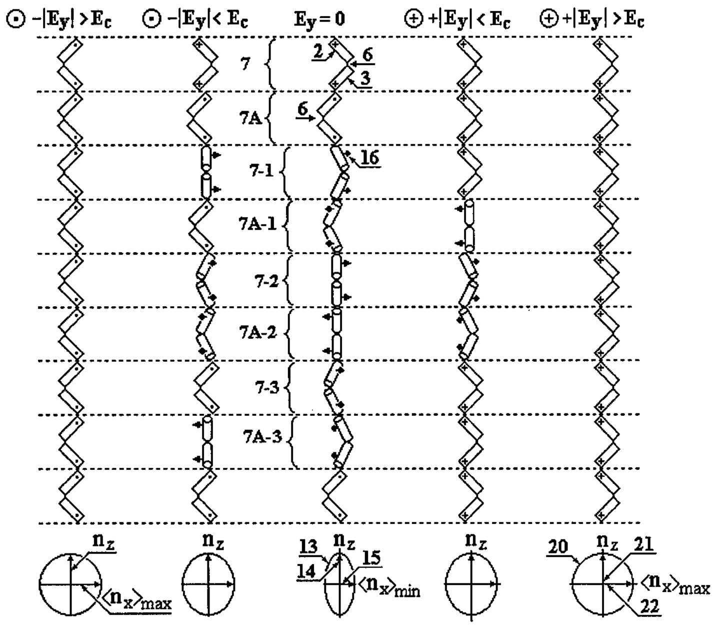

Fig.13. Antiferroelectric packing of neighbour smectic layers, composed from banana shape molecules.

In both cases the limit states, corresponding to different polarities of high enough electric voltages, are optically similar to each other, see Fig's 12, 13, left and right coulombs, only the directions of tips 6 are opposite. For small voltages, less than the threshold voltage of untwisting E_c , the gray scale takes place for the change of the refractive index component $<n_x>$, which varies from the value $<n_x>_{min}$ to $<n_x>_{max}$, Fig's 12, 13, at increase of voltage from 0 to $E_y > E_c$.

Phase modulation in the deformed helical smectic liquid crystal composed from banana shape molecules.

The ability of the proposed liquid crystal for phase modulation is related with the change of the refractive indices under influence of the electric field, applied along with smectic layers. The calculation of the refractive indices for the helical structure, composed from banana shape molecules, is based on the optical model of banana molecules as a sum of two equal refractive index ellipsoids 2' and 3', having the same value but opposite signs of the inclinations 4 and 5 of their long axes $n_{||}$, Fig.14.

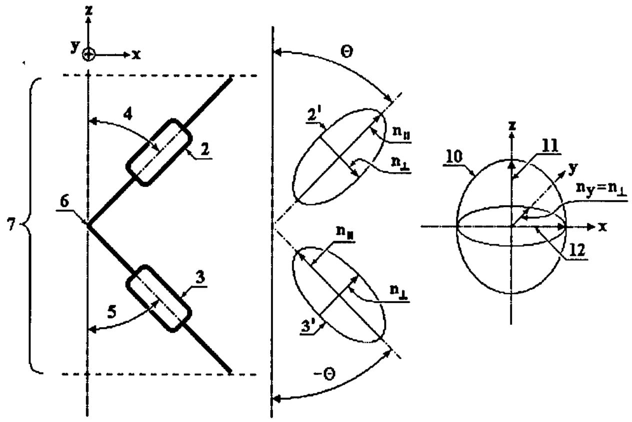

Fig.14. The optical refractive indices 2' and 3' of the constituent parts 2 and 3 of the banana shape (dimer) molecules, and the effective refractive index ellipsoid 10, describing the optical properties of the whole dimer molecule.

These refractive index ellipsoids 2' and 3' are related with the constituent parts 2 and 3, respectively, of the banana shape molecules 1, or dimers, shown in Fig's 11 and 14.

In case of the undisturbed helix the calculated refractive indices are similar to those for known helical smectic C structure, Fig.1, where the tilt angle 24 is equal to Θ, $n_{\parallel}$ and $n_{\perp}$ are the refractive indices along the axes of constituent parts 2 and 3, and perpendicular to them, respectively, Fig.14.

Refractive indices of bilayer structures from banana shaped molecules can be calculated using the method described above, if the refractive indicatrix of the molecules can be considered as the sum of the indicatrices of two subunits 1 and 2 with the same tilt angle but with $\varphi_2 = \varphi_1 + 180°$. The averaged refractive indices of the perfect helix is therefore identic with the usual DHF material with the same tilt angle θ. However, the totally unwound state is different. The optical axes don't change there direction and one finds (neglecting molecular biaxiality)

$$\begin{aligned} &< n_x > = n_{\perp} \\ &< n_y > = \sqrt{n_{\perp}^2 \cos^2\theta + n_{\parallel}^2 \sin^2\theta} \\ &< n_z > = \sqrt{n_{\perp}^2 \sin^2\theta + n_{\parallel}^2 \cos^2\theta} \ , \end{aligned} \tag{7}$$

where $n_{\perp}$ and $n_{\parallel}$ are the refractive indices perpendicular and parallel to the long axis of one sub-unit of the banana shaped molecule.

The upper limit for the modulation of the refractive index is given by the difference of the indices of the totally unwound state and the perfect helix. The only interesting index is n_y because n_z remains constant when an electric field is applied and the other varying index n_x is in direction of light propagation. The upper limit of $< \Delta n_y >$ can be calculated taking the relevant parts of equations 4 and 7, which gives

$$\begin{aligned} < \Delta n_y^{max} > &= < n_y > - < n_{\perp}^{helix} > \\ &= \sqrt{n_{\perp}^2 \cos^2\theta + n_{\parallel}^2 \sin^2\theta} - \sqrt{(n_{\perp 1}^2 \cos^2\theta + n_{\perp 2}^2 + n_{\parallel}^2 \sin^2\theta)/2} \end{aligned} \tag{8}$$

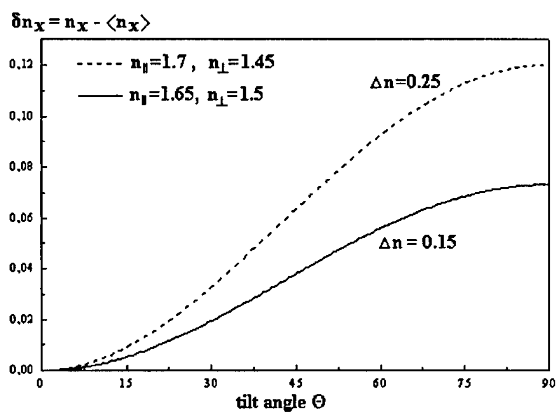

. The upper limit δn is plotted in Fig.15 versus the value of tilt angle Θ for two cases of the refractive indices of the sub-units 2 and 3 of dimers 1, namely 1) for $n_{\parallel} = 1.65$ and $n_{\perp} = 1.50$, and 2) $n_{\parallel} = 1.70$ and $n_{\perp} = 1.45$.

Fig.15. Upper limit for refractive index modulation as a difference δn_x between refractive indices n_x and $<n_x>$, correspoding to the untwisted state and nondeformed helix state of the smectic liquid crystal, composed from banana shape (dimer molecules). In Fig.1 the value δn_x corresponds to the difference between 22 and 15, Fig.11.

The upper limit for modulation of refractive index is given by the difference of indices describing the totally unwound state and the undisturbed helix. The index n_z remains constant and only change of the refractive index n_x takes place under influence of the untwisting voltage.

In Table 1 some numerical data are presented:

Table 1.

\refractive indicies Tilt angle θ \	$n_{\|} = 1.65; n_{\perp} = 1.50$	$n_{\|} = 1.70; n_{\perp} = 1.45$
20	0.0091	0.015
25	0.013	0.023
30	0.019	0.032
35	0.025	0.042
40	0.031	0.053
42	0.034	0.057
45	0.037	0.063

For the totally untwisted state, shown in right part of the Fig.11 the optical axes do not change their direction and one finds in neglection of the molecular biaxiality:

$n_y = n_{\perp}$; $n_x = (n_{\perp}^2 \cos^2\Theta + n_{\|}^2 \sin^2\Theta)$; $n_z = (n_{\perp}^2 \sin^2\Theta + n_{\|}^2 \cos^2\Theta)$;

In Fig.16 the effective refractive indices n_y n_x and n_z are plotted for the untwisted state of the structure, presented in right part of Fig.11 . Here the refractive indices $n_{\|}$ and $n_{\perp}$ of sub-units 2 and 3 of banana molecules 1 are chosen as following: $n_{\|} = 1.65$ and $n_{\perp} = 1.50$.

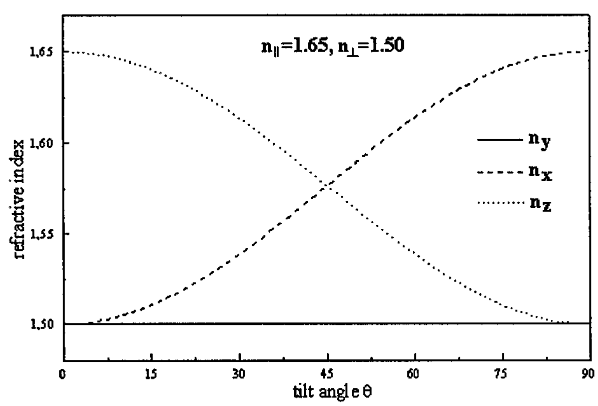

Fig.16. The dependence of the refractive index components n_y, n_x (component 12 in Fig.5), and n_z (component 11 in Fig.5) of the smectic liquid crystal, composed from banana shape molecules at totally untwisted helix, on molecular tilt angle Θ.

The gray scale behaviour of the refractive index n_x under influence of electric field in deformed helical structure of the banana shape molecules.

In general, the local dielectric tensor of the bilayer structure depending on the angle φ is as follows:

$$\varepsilon_{11}^{loc} = \varepsilon_{\perp} \cos^2\theta \cos^2\varphi + \varepsilon_{\perp} \sin^2\varphi + \varepsilon_{\|} \sin^2\theta \cos^2\varphi$$

$$\varepsilon_{12}^{loc} = \varepsilon_{21}^{loc} = (-\varepsilon_{\perp} \cos^2\theta - \varepsilon_{\|} \sin^2\theta + \varepsilon_{\perp}) \sin\varphi \cos\varphi$$

$$\varepsilon_{22}^{loc} = \varepsilon_{\perp}\cos^2\theta\sin^2\varphi + \varepsilon_{\perp}\cos^2\varphi + \varepsilon_{\parallel}\sin^2\theta\sin^2\varphi \quad (8)$$
$$\varepsilon_{22}^{loc} = \varepsilon_{\perp}\sin^2\theta + \varepsilon_{\parallel}\cos^2\theta$$

These equations can again be used to calculate the indicatrix in dependence on the electric field according to the model described above. The results of calculations for two different sets of molecular indices are shown in the figure 17 for the case of a tilt angle θ=40°.

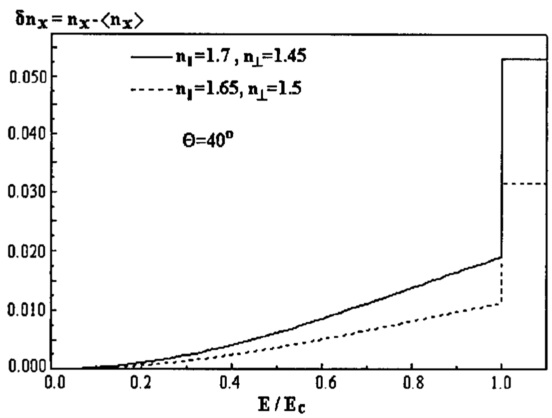

Fig.17. The increase δn_x of the refractive index component from its initial state $\langle n_x \rangle$ under increase of the electric field for two sets of refractive indices, describing the constituent parts 2 and 3 of dimer molecule 1. Tilt angles 4and 5 in Fig.12 are equal to Θ = 40°.

Very good gray scale in variation of n_x versus voltage is seen. The amplitude of the gray scale in $n_x(E)$ is almost proportional to the molecular tilt angle Θ, and for Θ=40...45° the maximum change of n_x reaches 0.02, Fig.18.

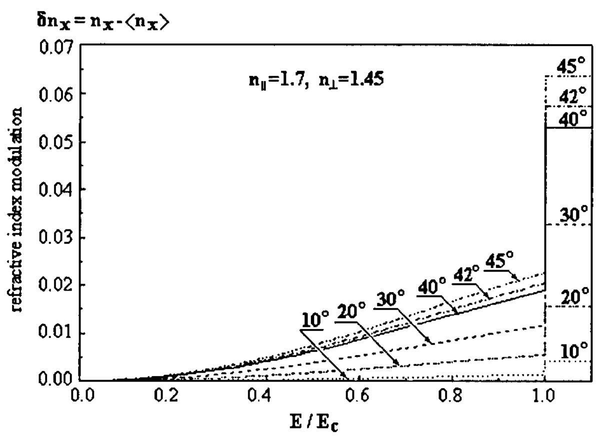

Fig.18. The same as in Fig.17 for different angles of inclination of long axes of subunits 2 and 3, Fig.14.

It means that perfect gray scale for phase shift 2π of light wave with λ=0.63μm will be at cell thickness of the order 30μm. Using the double passing of the light beam through the cell by means of mirror behind of cell, as it is shown for instance in Fig.30, the necessary thickness will be two time less, about 15μm. In regime of bistable switching between states with the phase difference 2π, for electric field E_y, exceeding the threshold value E_c , the change of the refractive index n_x reaches 0.053...0.063. It means that thickness of the FLC cell can be reduced to 10μm in transmissive mode and to 5μm in reflecting mode of phase modulator.

2.1.4. The chemical realization of the proposed liquid crystal.

Cenral cores 2 and 3.

These fragments of the proposed liquid crystal can be chosen from any known ciclic fragments, used so far for the synthesis of liquid crystals. Commonly used phenyl, penyl-pyrimidine, pyridine, terphenyl, biphenyl, biphenyl-pyrimidin and any another aromatic and/or polyciclic fragments can be used to provide the optically anisotropic central cores 2 and 3, characterized by parallel and and perpendicular refractive index components $n_{\parallel}$ and $n_{\perp}$, Fig.5.

Spontaneous polarization and molecular chirality.

To realize the low voltage control of the azimuth 8, 9 of the tips 6 of the banana shape molecules 1, the proposed molecules apart from central cores 2 and 3, responsible for the optical properties in visible range of spectrum, have the chiral fragment 39, Fig.19, which contains the dipolar moment 16.

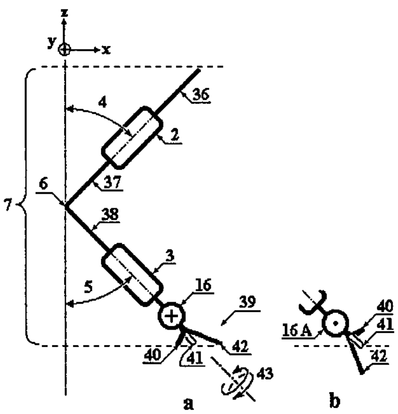

Fig.19. The banana shape dimer molecule, composed from two constituent central cores 2 and 3, responsible for optical properties in visible range of spectrum, and from alyphatic chains 36, 37, 38, and from chiral fragment 39, formed by tripod of molecular tails 40, 41, 42 of different length. The preferable orientation of the transverse dipolar moment 16 does occur owing to the hindrance of the molecular librations 43 around long axis of the constituent part of dimer, described with fragments 38+3+16+39.

If such molecule is embedded into smectic layer 7, the dipole moment 16 will be directed in certain direction y owing to the hindrance of the librations of molecule along their long axis , connecting the tip 6 and chiral fragment 39. This hindrance has the same nature as it was described by R.B.Meyer et al [8] and is related with the monoclinic surrounding near the chiral fragment 39, composed from molecular tails 40, 41 and 42, having the different lengths, usually formed by three different aliphatic and fluorinated fragments, like

$$-C^*H(CH_3)C_nH_{2n+1} \text{ or } -C^*H(CF_3)C_nH_{2n+1}$$

where n=2…8, the mostly preferable n=3…6. The state (a) of such molecule is more preferable than the state (b). The dipolar moments 16, attached to the chiral fragment 39 will have the transverse component along the normal to inclination plane, or along the y axis in Fig.19. The dipole moments can be realized by different polar molecular groups, like -CO-O-, -CO, $-CF_3$ and many another.

The polyphilic approach to the design of the banana shape dimer molecules to prevent the cancellation of the spontaneous polarization for dimers.

If the dimer molecules are composed from two central cores 2 and 3, from aliphatic chains 36, 37, 38, and chiral fragment 39, with the dipole moment 16, the mutual cancellation of the spontaneous polarization induced by two molecules in smectic layer will takes place. It is connected with the presence of the two equal possibilities for arrangment of the discussed molecules within the same smectic layer, Fig.20. The 50% of molecules will have the orientation of the chiral fragments in the position 39, and 50% of mlecules will have the orientation of chiral fragments in the position 39'. The dipole moments 16 and 16', respectively, will have the opposite signs, inducing the compensation of the macroscopic spontaneous polarization.

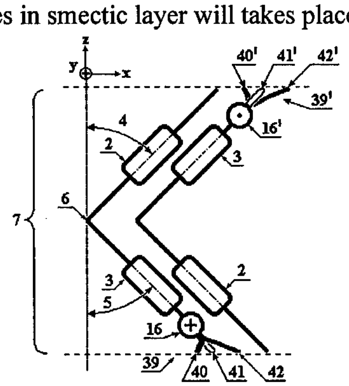

Fig.20. The cancellation of the spontaneous polarization within smectic layer due to simmetrical packing of two oppositely oriented molecules. Dipoles 16 and 16' have opposite directions.

To avoid this cancellation effect, we propose to introduce the special fragment 44, based on perfluorinated chain, into banana shape molecules composed from two central cores 2 and 3, Fig.21 .

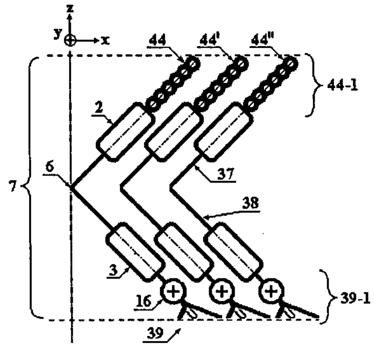

Fig.21. The proposed structure of the polyphilic chiral banana shape molecules, which form the smectic layers with the noncancelled spontaneous polarization.

The tail 44 is formed for instance with the perfluorinated chain ($-CF_2-)_n$, which replaces the alyphatic hydrocarbon chain 36 of the molecule, shown in Fig.19. Such tails do form the mutual packing within layer 44-1. It prevents to the cancellation of the spontaneous polarization in smectic layer 7. Dipole moments 16 of all molecules in smectic layer are directed in the same direction along y-axis.

The perfluorinated fragment can have the following structure : $-(CF_2)_n-$, where n=4...16.

Such fragments, being introduced into the dimers 1 instead of one aliphatic, e.g. hydrocarbon chain $-(CH_2)_n-$, for example instead of chain 36, provide the strong polyphilic segregation of the molecular fragments within smectic layer, as it was discovered by Tournilhac et al [23, 24] for non-dimer compounds with the structures, presented in Table 1, where the data are given about tilt angles for the central core (optical tilt angle Θ_{opt}) and about tilt angles of the inclination of perfluorinated chain relative to the normal to smectic layers (fluorinated tail tilt angle Θ_F):

Here the abbreviature Φ designates the phenyl ring  and $_N\Phi$ designates the pyridine ring 

Table 2. Examples of smectic C liquid crystals with fluorinated chains [23, 24].

Material	Optical tilt angle Θ	Fluorinated tilt angle Θ_F
$F(CF_2)_8(CH_2)_{11}$-O-Φ-Φ-CN	48	28
$F(CF_2)_8(CH_2)_{11}$-O-Φ-$_N$Φ-CN	49	30
$F(CF_2)_8(CH_2)_{11}$-O-Φ-Φ-CO-O-CH_2CF_3	51	33
$F(CF_2)_8(CH_2)_{11}$-O-CO- Φ-Φ-O-CH_2CF_3 [19]	n.a.	n.a

From X-ray data it was found [24] the strong segregation of fluorianted chains and formation of the sub-layers , consisting of these chains. According to our proposal this property of the fluorinated chains will prevent to the packing of the molecules, shown in Fig.20. The proposed smectic phase structure will have no compensation of the dipole moments 16, owing to the segregation of the fluorinated chains, as it is shown in Fig.21. The fluorinated chains 44, 44', 44"etc., do form the sub-layer 44-1, preventing to the flip-flop orientations of molecules within one smectic layer 7. As a consequence the chiral fragments 39 will be collected in another sub-layer 39-1 within the same smectic layer 7. The simmetry of this sub-layer allows one to the summarization of the transverse dipole moments 16 near the chiral fragments 39 in the same direction y.

The another advantage of the fluorinated chains is connected with the higher optical tilt angle Θ_{opt} of the order 45° or more, see Fig.22 and Table 1, also the Ref.[25], in comparison with analogous smectic liquid crystals with hydrocarbon chain instead of perfluorinated chain.

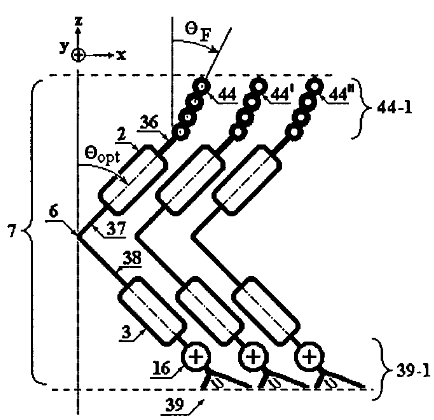

Fig.22. The polyphilic molecules with the perfluorinated chain 44 connected to the aliphatic hydrcarbon tail 36 outside of central core 2.

The fluorinated tilt angle Θ_F is much less than Θ_{opt}, that is related with the larger area (27Å^2) of the cross-section of this chain in comparison with cross-section of hydrocarbon chain (22Å^2). The fine fitting of the angle Θ_{opt} can be made by means of the ratio of lenght of molecular chain 44 to length of chain 36 as it was described in [25].

The additional advantage of the perfluorinated chain is the appreciable decrease of the rotational viscosity of the ferroelectric liquid crystal, and the decrease of the response time can be obtained shorter than 15 microseconds [25]. Due to the chirality of the molecules, connected with the presence of the chiral fragments 39 the directions of tips 6 in electric field free state will form the helical structure, shown in Fig.11, left part, with the uniform change of the azimuthal angles 8, 9, etc.

In Appendix the different versions of the molecular structure are presented, depending on the position of the perfluorinated chain and number of chiral fragments.

3. Development of DHF materials.

In this work the ferroelectric liquid crystal materials possessing the DHF (deformed helix ferroelectric) effect have been developed with assembly of optimized characteristics for applications. These materials were made on the basis of blends of inclined smectic C matrix and chiral additives, inducing the helical structure and spontaneous polarization. The substances from phenyl-pyrimidines and ether derivatives of biphenyls and terphenyls were used, see Fig. 23.

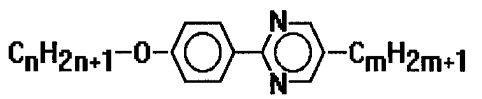

n, m = 5÷9

$Cr \xleftrightarrow{18} S_C \xleftrightarrow{46} S_A \xleftrightarrow{56} N \xleftrightarrow{63^oC} I$ (n=6, m=8)

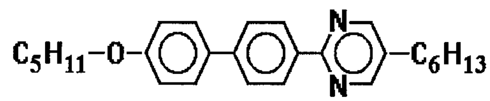

$Cr \xleftrightarrow{44} S_C \xleftrightarrow{79} N \xleftrightarrow{158^oC} I$

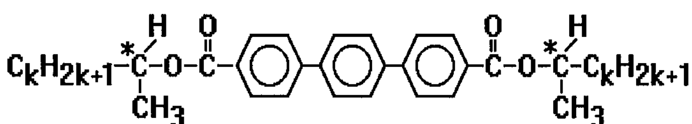

k = 3, 4, 6

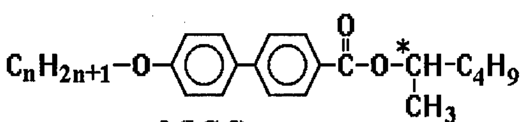

n=6, 7, 8 n=8 (LG-8)

Fig. 23. Basic chiral and achiral compounds used for development of ferroelectric liquid crystal materials.

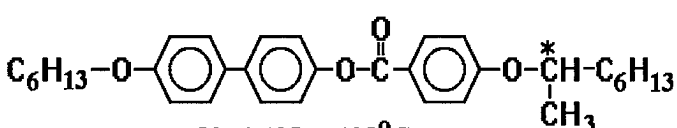

VG-8 $Cr \xleftrightarrow{89} S_C^* \xleftrightarrow{105} N \xleftrightarrow{128^oC} I$

In Table 3 the data about some developed DHF materials are presented.

Table 3. Parameters of the developed DHFmaterials

FLC material Parameter	FLC-464	FLC-471	FLC-474
Interval of smectic C* phase	+5…+62°C	+2…+62.5°C	-5…+52°C
Tilt angle (+25°C)	40°	39.5°	31°
Spontaneous polarization, nC/cm^2 (+25°C)	120	115	190
Pitch of helix, μm (+25°C)	0.18	0.19	0.26
Response time, μs (+25°C)	500	500	250

In Interim Report 1 three groups of the developed DHF materials and their basic parameters are described. The substances of second group seemed to be the most suitable for further application in designing the different electrooptical devices. These mixtures have very large tilt angle of the order of 40° and very small pitch of helix less than 0.2μm, see Table 3, FLC-464 and FLC 471. The characteristic relaxation time of deformed helix effect was less than 1ms. In Fig. 24 phase diagram for set of such mixtures is presented, and in Fig.25 the temperature dependences of spontaneous polarization and of tilt angle are plotted.

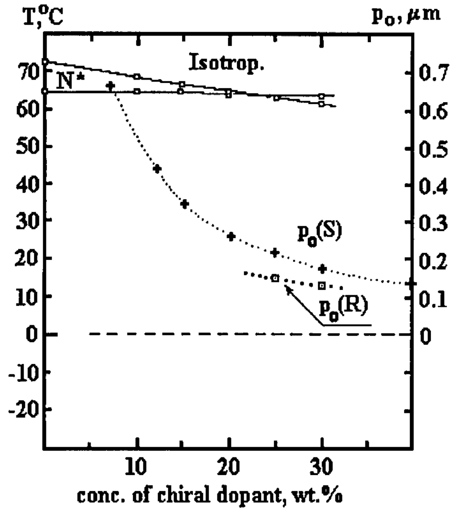

Fig.24. Phase diagram of DHF materials with large tilt angle Θ_0 and short pitch of helix p_o. Tilt angle Θ_0 of chiral matrix above 42°, chiral dopant (S)Luch induces the helix with pitch 0.18...0.22μm at 25-30w.%. The chiral dopant with opposite sign of chirality (R)Luch induces even shorter pitch 0.16...0.14μm

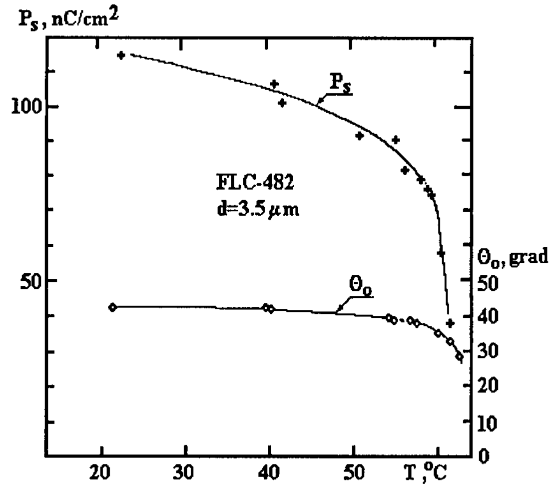

Fig.25. Temperature dependence of spontaneous polarization P_s and tilt angle Θ_0 for DHF material FLC-482. Pitch of helix p_o =0.2μm at T=25°C.

3.1. Measurements of refractive indicies.

In Table 4 we present the data about refractive index component $< n_{\parallel} >$ along the normal to smectic layers and $< n_{\perp} >$ along the smectic layers. The concentration of chiral dopants c_d, transition temperature T_{CA} between smectic C* and smectic A phases, as well as effective anisotropy of refractive index $< \Delta n > = < n_{\parallel} > - < n_{\perp} >$ and sum of indicies $\Sigma = < n_{\parallel} > + < n_{\perp} >$ are also presented.

Table 4.

FLC	c_d, wt%,	T_{CA}, °C	$< n_{\parallel} >$	$< n_{\perp} >$	$< \Delta n >$	Σ
472	40.2	3	1.6585	1.4828	0.176	3.141
355	40	17	1.6593	1.4834	0.176	3.143
374	40	16.5	1.6592	1.4845	0.1747	3.144
356	40	28	1.6530	1.4846	0.167	3.139
370	44.0	30.6	1.6536	1.4900	0.1636	3.144
369	44.0	31.0	1.6540	1.4903	0.164	3.144
448	47.0	27.3	1.6661	1.4862	0.180	3.152
447	48.0	30	1.6642	1.4870	0.177	3.151
247	40.4	52.8	1.6184	1.4994	0.119	3.118
248	40.3	59.6	1.6186	1.5015	0.117	3.120
277	46.8	55.2	1.6242	1.5053	0.119	3.130
474	50.6	52	1.6234	1.5040	0.119	3.127
473	31.3	63	1.5959	1.5140	0.082	3.110
456	10	68.5	1.5923	1.5269	0.065	3.1192
459	15	66.5	1.5897	1.5164	0.073	3.1061
460	20	65	1.5895	1.5135	0.076	3.103
461	25	64	1.5905	1.5124	0.0781	3.1031
473	31.3		1.5946	1.5128	0.0818	3.1074
469	35		1.6000	1.5134	0.0866	3.1134
468	40		1.6012	1.5124	0.0888	3.1136

The refractive indicies were measured using standard Abbe refractometer for yellow light line 589nm. The parallel and perpendicular components were measured using polarized light along the normal to smectic layers and perpendicular to this normal, resp. In Interim Report 1 the measured values are plotted in Fig's 10 and 11. The data about refractive coefficients allow us to estimate the limit phase modulation in DHF materials as a difference of sums $\Sigma = < n_{\|} > + < n_{\perp} >$ between data related with untwisted state and nondeformed helix state, see Interim Report, pp.2-3.

4. Preparation of experimental DHF modulators.

Different techniques were developed for the fabrication of modulators on the basis of developed DHF materials. The rubbed polymer polyvinyl alcohol film was used in some cases as an orienting layer. The spin-coating machine was designed for preparation of such films where the parameters of spin-coating and rubbing procedures were strongly controlled (rotation speed, time of spin, concentration of polymer, pressure of solvent vapors, further etching and rubbing, etc.). The vacuum chamber was designed to avoid the appearance of air bubbles after filling the capillary gap with liquid crystal. For enhanced optical uniformity the modified shear technique was used with simultaneous application of a.c. voltage. The thickness of FLC layer was controlled by teflon or mylar spacers and was measured using interference technique. The majority of samples were made using the glass and quartz substrates with diameter 35mm, acquired in PeterLab, Ltd, St.Petersburg, Russia. These substrates were covered with necessary coatings like ITO (indium-tin-oxide) electrodes, smooth and protecting HfO_2 layers, photoconducting layers on the basis of amorphous hydrogenited silicon carbide a-Si:C:H or of quasi-amorphous zinc selenide ZnSe. Examples of the fabricated electrically as well as optically addressed modulators are presented in Fig's 26, 27. In Interim Report 1 the samples of double DHF modulator are also shown, see Fig's 14, 16 therein.

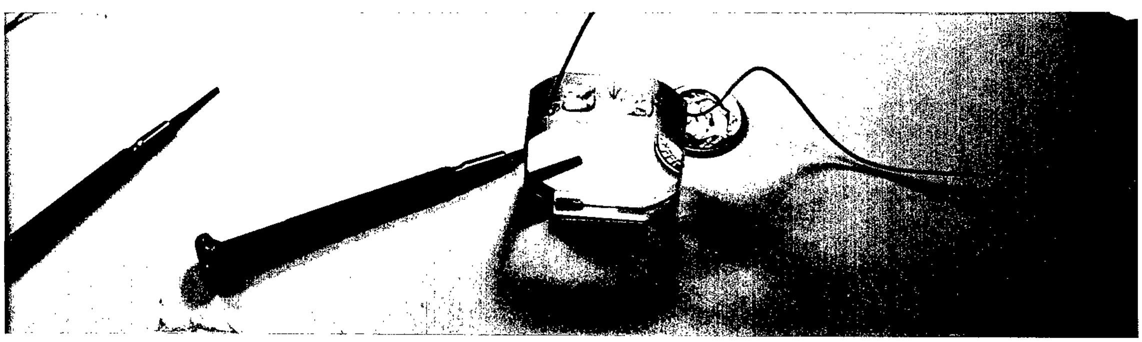

Fig.26. Single pixel electrically addressed DHF modulator for design of double DHF phase modualtor and for measurements of basic physical parameters. At some angle of observation the blue diffraction is visible revealing the very short pitch of helix.

Fig.27. Optically addressed spatial light modulators utilizing the developed DHF materials. Left - OASLM for trasmissive mode of red read out light, middle and right - for reflective read out mode.

4.1. Mesurements of phase modulation using the double DHF modulator.

The operation of phase modulator, composed from two crossed DHF cells, discussed in section 2.1.2, was tested in Fizeau interferometer, shown in Fig. 13 of Interim Report 1. In Fig.28 the shift of interference pattern in dependence on applied d.c. voltage was presented for modulator, composed from two crossed DHF cells, similar to shown in Fig.26. DHF material FLC-482 was used for both cells. Thickness of FLC layers was 16.5 μm.

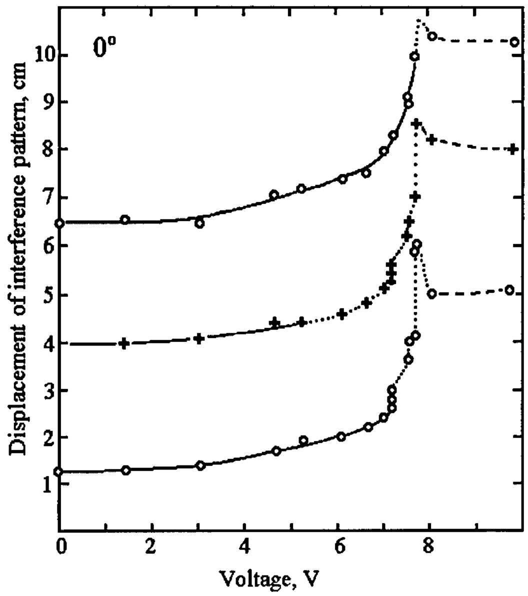

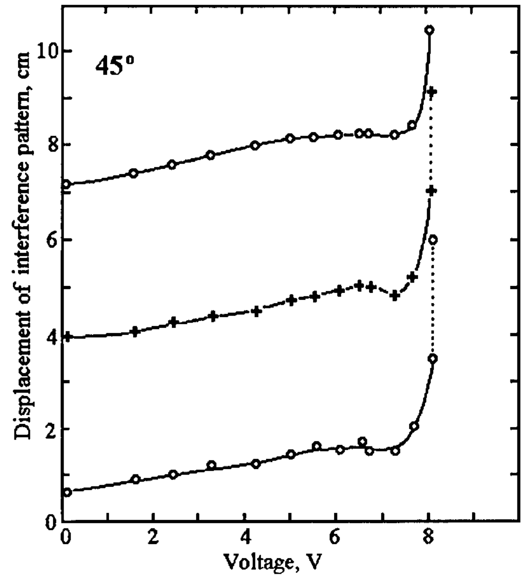

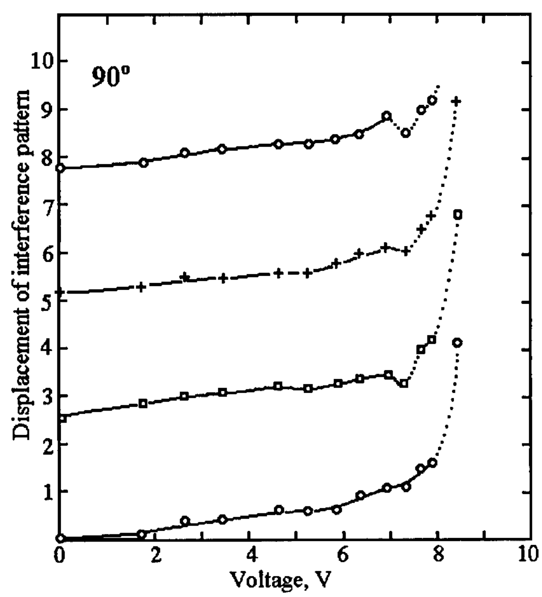

Fig.28. The displacement of the interference strips observed in Fizeau interferometer for phase modulator composed from two crossed DHF cells with thikness 16.5μm. Dependence on applied d.c. voltage. Three orientations of polarization plane relative to helical axis of the input cell are used. The displacement is measured on the monitor screen, connected with video camera , recording the interference pattern, see Fig.13 of Interim Report 1.

Basic features of the found experimental data do agree with the calculations presented in section 2.1.2, see Fig.9. At first there are no significant dependence on light polarization. At second the gray scale versus applied voltage is available in range of DHF regime. At third, the very nonlinear increase of effective refractive index is characteristic of this modulator in total agreement with Fig.9. At voltages close to the values of helix untwisting the almost jump transition to the effective refractive index $n_{eff} = n_{\|} + n_{\perp}$ of the unwound state is observed.

The limit phase modulation calculated from difference between effective refractive indicies in untwisted and nondeformed helix states agrees with calculations within 15%, see Interim Report 1, p.3, paragraph 4.

5. Development of the optically addressed spatial light modulator using large tilt angle DHF material for real-time holography and adaptive optics applications.

The developed DHF materials with large tilt angle and short pitch of helix appeared to be very suitable as a light phase modulating media in optically addressed spatial light modulators. The basic reason of greate perspective of such materials is the fact that any polarization of light beam will interfere with high diffraction efficiency on phase diffraction grating composed from uniaxial optical plates with interchanging deviations of their slow optical axes [26]. Earlier we have shown the switchable phase diffraction grating , using computer controlled voltage distribution on one dimensional array of narrow FLC cells with period 25μm [27] .

In ideal case of deviation angle +/- 45° in neighbour uniaxial plates, Fig.29, the diffraction efficiency for non-polarized light will be about 40% [26]. In case of the our developed FLC mixtures we have the switchable tilt angle $\Theta_0 = 40°$ that is close to the 45°. Optically addressed spatial light modulator utilizing such material was assumed to have much higher diffraction efficiency in comparison with OASLM utilizing the standard SSFLC (surface stabilized ferroelectrtic liquid crystal [9]) mixtures with the switchable tilt angle $\Theta_0 = 22\text{-}25°$ [28,29].

We have fabricated the OASLM utilizing the DHF materials with large tilt angle and they were tested in different optical schemes in Darmstadt University of Technology, Germany [30], in Institute of Laser Physics, St.Petersburg, Russia [31, 32], in Air Force Philips Lab, Albuquerque NM [33] and in Army Research Lab., Adelphi MD [34]. The high figures of merit for basic parameters were obtained in holographic techniques of diffraction efficiency meaurements and correction of severe aberrations of optical systems [30-34]. The detail description of the development of mentioned OASLM's and their investigation were presented to conferences and submitted for publications.

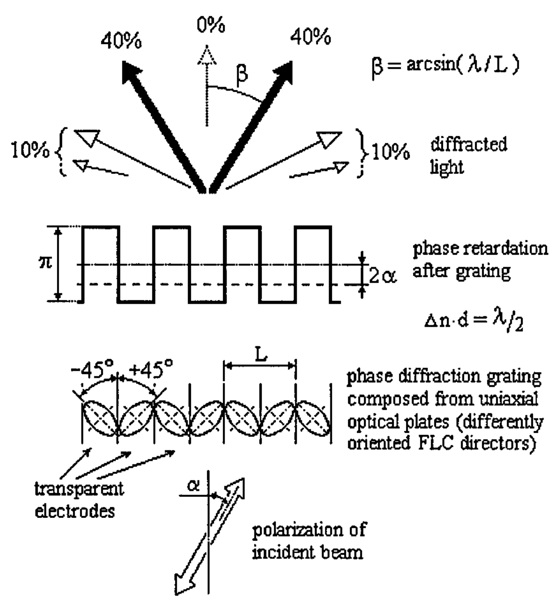

Fig.29. The polarization non-sensitive diffraction of light beam from phase diffraction grating composed from uniaxial optical plates. Thickness of plates d, refractive index anisotropy Δn, light wavelength λ. Thickness of plates satisfies to condition $\Delta nd = \lambda/2$.

6. Testing of low viscous nematic liquid crystal with high refractive index anisotropy for fast phase modulation.

Having in mind the well developed optical and electronic schemes in Army Research Laboratory for use and control of multi-pixel electrically addressed spatial light modulators based on nematic liquid crystals, like LC television panel and Meadowlark SLM "Hex127", the testing of the improved nematic liquid crystals was made. We have used the nematic liquid crystal with large refractive index anisotropy $\Delta n = 0.27$ for $\lambda = 589$nm and have found the possibility of operation rate till 60Hz for phase modulation depth equal to $\lambda = 633$nm if cell thickness d=3.5μm and reflective cell is used (two passing of modulated beam through the liquid crystal layer , see Interim Report 2, p.3, Fig's 7,8,9.

7. Two frequency addessed nematic liquid crystals for fast phase modulation.

It is known that nematic liquid crystals with sign change of dielectic anisotropy can be used for so called two frequency addressing method of driving. At relatively low frequency 0.5-1 kHz such material has the positive dielctric anisotropy $\Delta\varepsilon > 0$ and applied voltage with such frequency does reorient the nematic director from planar alignment to hometropic state with response time of the order of millisecond or parts of millisecond. When the voltage is switched off the slow relaxation to the initial planar orientation takes place with chatacteristic time of the order of tens and hundreds millisecond, depending on cell thickness and visco-elastic parameters of liquid crystal, see Fig.8, Interim Report 2. The reorientation of nematic director can be strongly reduced by applying the high frequency voltage. In this case the dielectric anisotropy is negative $\Delta\varepsilon < 0$ and applied voltage forces to align the nematic director parallel to electrodes. In Fig. 30 the scheme of the reorientation process in two frequency nematic liquid crystal is presented with characteristric parameters of applied voltage and response times.

We have prepared the one pixel cell with nematic liquid crystal ZhKM-1001 having the following parameters:

- dielectric anisotropy $\Delta\varepsilon$, 500Hz - +2.3
- dielectric anisotropy $\Delta\varepsilon$, 40,000kHz - -2.3
- inversion frequency, kHz - 7
- optical anisotropy, 589nm - 0.25

The planar orientation of this liquid crystal was made in capillary cell with thickness 5.4μm, using the rubbed polyvinyl alcohol film as aligning layer. The set-up for meaurements of response time of cell was the same as in Fig.7 of Interim Report 2. The S-effect in this case shows again the pure phase modulation for light polarization along the nematic director. The characteristic response oscillograms are presented n Fig.31. For relatively moderate driving conditions: -amplitudes of sine-wave voltage +/-28V at frequncies 1kHz ($\Delta\varepsilon>0$) and at 20kHz ($\Delta\varepsilon<0$) the whole circle of phase modulation in range 0-π was obtained during the time interval 4ms. It means that operation frequency can be in range 250Hz. The phase modulation depth 0-2π can obtained at the same condition using the reflective type of modulator. It is possible to receiving higher phase modulation (0-2π) in transmissive modulator by increasing the amplitude of voltage or/and cell thickness.

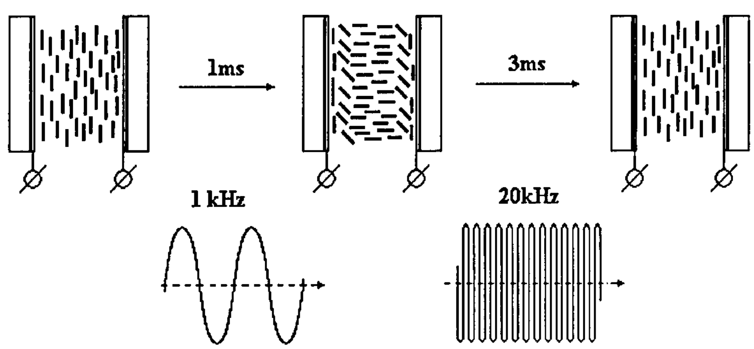

Fig.30. The scheme of two frequency controlled reorientation of nematic liquid crystal for phase modulation (S-effect).

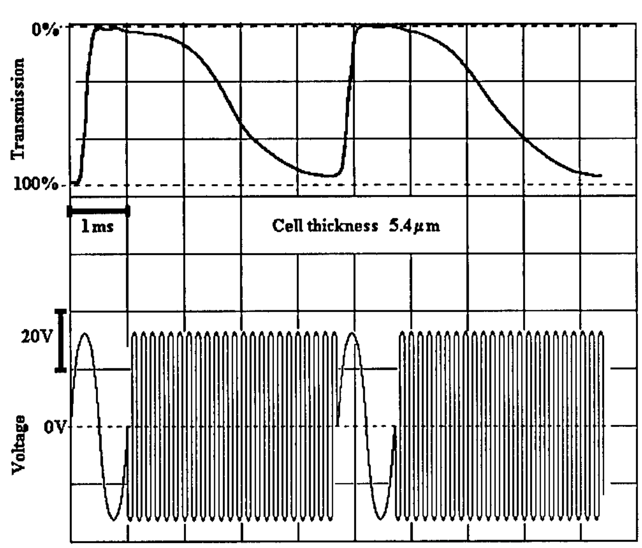

Fig.31. The response oscillogram of nematic liquid crystal with change of sign of dielectric anisotropy. The low frequncy is 1kHz, the high frequency is 20kHz. Cell thickness 5.4μm. Nematic liquid crystal ZhKM-1001 (NIOPIC, Moscow, Russia).

8. The design of mosaic electrically addressed spatial light modulator for low viscous and two-frequency addressed nematic liquid crystals with high refractive index anisotropy.

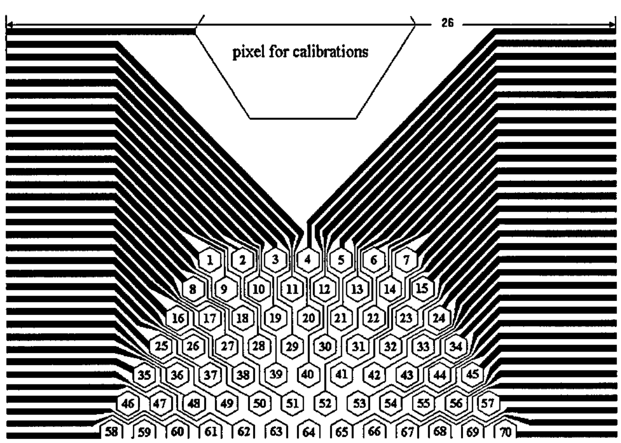

To realize the possibility of fast phase modulation in real optical systems based on wave front correction we have made preliminary steps for fabrication of mosaic multipixel electrically addressed modulator with 127 independently controlled pixels. The draft of photomask for preparation of substrates with transparent ITO pixelized electrodes is presented in Fig.32.

Fig.32. The draft of upper part of multipixel modulator with independently controlled 127 pixels.

The size of one pixel is 1mm. The diameter of working aperture about 13mm. The whole diameter of substrate 35mm. The bottom part is almost symmetrical to shown in this Figure. The inner part of modulator is similar to that designed by Meadowlark Optics. The outer part is designed for shortest electrical connection to computer through the connecting card, Fig.33.

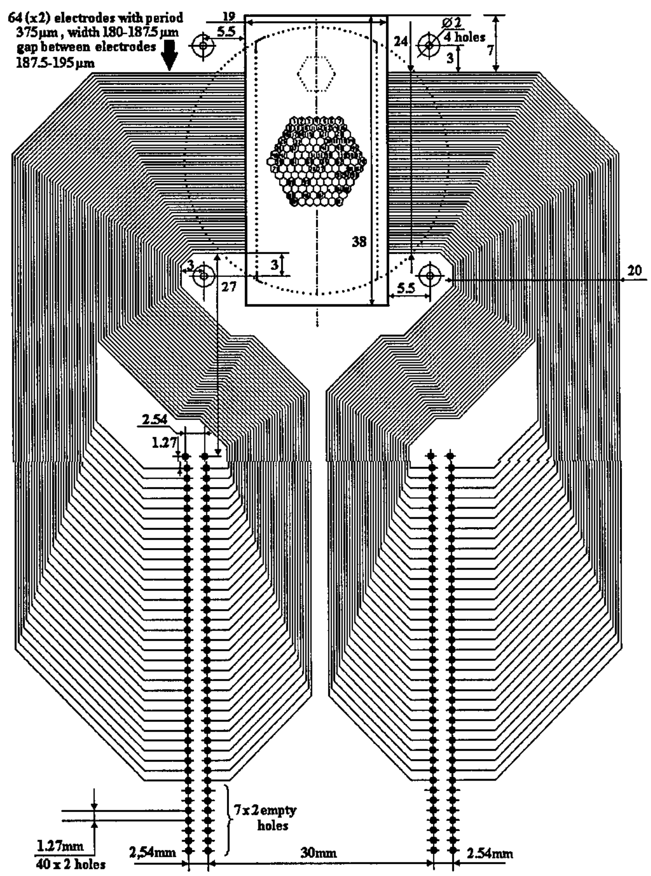

Fig.33. Interface card for connecting the modulator with 127 pixels, outer diameter 35mm, with cables for further connection with computer

This card-interface will allows us to use the elelectronics, hardware and software, developed in Army Research Laboratory together with Johns Hopkins University MD.

Conclusions:

1) Ferroelectric liquid crystal materials are developed possessing the DHF (deformed helix ferroelectric) effect with optimized characteristics for design of light phase, polarization and intensity control in room temperature range. Materials have variable tilt angle 30-39.5°, pitch of helix 0.18-0.35mkm and spontaneous polarization 100-150nC/cm^2 . Materials are characterized by short respoinse time 0.5-1ms. The averaged refractive indicies are measured for helical nondisturbed structure as well as componets of molecular refractive index for ortogonal smectic A phase.

2) Electrically controlled one pixel DHF cells are designed and fabricated and phase modulator was designed on the basis of two crossed DHF cells. The phase modulation of this device was measured by interferometer technique in dependence on applied d.c. voltage. The limit phase modulation was calculated for crossed DHF cells and experimental results are in good agreement with calculations.

3) The optically addressed spatial light modulators (OASLM's) were developed for dynamical holography and adaptive optics applications utilizing the deformed helix ferroelectric (DHF) liquid crystals with large tilt angle 39-40° , with short pitch of helix of the order of 0.2 microns and less, and with response time less 1ms. As a photoconductors a-Si:C:H and dye-dopped polyimide films are used. The first is most suitable for fast (hundreds Hz) OASLM's, with moderate resolution of the order 10^2 lp/mm and with controlled transmission spectum owing to the possibility to shift the absorbtion band by means of variation of carbogen content. Polymer photosensor provides the highest spatial resolution upto many hundreds lp/mm at real time of OASLM operation in range of second and part of second.

At moderate intensities of light pulses around 100-300microWatt/cm^2 the light deviated optical axis of FLC layer reaches 50-55°. High diffraction efficiency (DE) 20% was obtaiend, related with the large amplitude of the phase variation exceeding 112° in the liquid crystal phase diffraction grating (hologram) in holographic application. This value of DE was obtained for OASLM's utilizing the both mentioned photoconductors.

In transmissive OASLM's the spatial resolution is of the order of 100 lp/mm at the level of MTF (modulation transfer function) 50%. The threshold sensitivity of OASLM's, using α-SiC:H (i) films and DHF materials is of the order of 10^{-7} W/cm^2. For α-SiC:H films in p-i-n configuration the threshold sensitivity can be of the order of 10^{-8} W/cm^2. The response time of OASLM's, using α-SiC:H (i) films and DHF materials, are of the order of 1-2ms.

3) The thin optically black film of the amorphous hydrogenited carbogen α-C:H was firstly used as a light blocking layer in combination with amorphous hydrogenited silicon carbide α-Si:C:H. Transmission in visible range is less than 1% at thickness of film of the order of 1 micron, resistivity is variable in range 10^8-10^{12} Ohm.cm. at. This film provides the possibility to design optically addressed phase modulators of reflective type, using the thin dielectric or metal pixelized mirror. The reflective type of OASLM has strong advantage in case of using the nematic liquid crystal owing to the smaller thickness of the liquid crystal layer and much shorter relaxation time for the same phase modulation in comparison with transmissive OASLM's.

5) The developed OASLM's utilizing the FLC with large tilt angle were succesfully applied for correction of severe aberrations in the telescope system.

6) The new molecular approach was suggested for the synthesis of the ferroelectric liquid crystals for phase modulation. The banana shape dimer structure of the molecules , consisting of two oppositely inclined central molecular cores, do form the smectic phase with strongly twisted helical structure. The ferroelectric as well as antiferroelectric packing in the neighbour smectic layers, provide the gray scale phase modulation, if the pitch of helix p_o is less than wavelength λ. The phase shift λ (one wavelength) can be achieved in gray scale mode in the cell thickness of the order of 25 microns, transmissive mode, and around 12 microns in reflective mode. The different variations of the chemical realization of the suggested dimer banana shape molecules, forming the smectic helical structure, are considered.

7) The nematic liquid crystals with very large refractive index anisotropy $\Delta n \approx 0.27$ were tested for the phase modulation with enhanced operation rate. In the reflective device the gray scale phase modulation with the control of phase shift λ is estimated in range of 75Hz.

8) Two frequency controlled nematic liquid crystal was tested for fast phase modulation using material ZhKM-1001 with change of sign of dielectric anisotropy. The time 4ms of total switching circle between two phases in range 0-π was obtained. It allows us to design the electrically addressed spatial light modulators with operation rate of the order of 200Hz.

9) The substrates with 127 transparent electodes and interface card connecting the OASLM with computer are designed for preparation multipixel electrically addressed spatial light modulators, using high optical anisotropy nematic liquid crystals and nematic liquid crystals with change of sigh of dielectric anisotropy.

Presentation and publication of results:

1. "Novel liquid crystal spatial light modulators for adaptive optics and image processing" by A. P. Onokhov, V. A. Berenberg, A. N. Chaika, N. L. Ivanova, M. V. Isaev, N. A. Feoktistov, L. A. Beresnev, and W. Haase, presented to SPIE's 12 Annual Int. Symp. "AeroSense", section "Advances in Optical Information Processing VIII", 13-17 April 1998, Orlando, Florida USA, Advanced Technical Program, p.52. Published in Proceedings of SPIE, Vol. 3388.
2. "Polychromatic correction for aberrations in the lenses of telescopic systems using liquid-crystal optically addressed spatial light modulators", by V. A. Berenberg, M. V. Vasiliev, V. Yu. Venediktov, A. A. Leshchev, L. N. Soms, A. P. Onokhov, L. A. Beresnev, and W. Haase, presented to SPIE's 12 Annual Int. Symp. "AeroSense", section "Advances in Optical Information Processing VIII", 13-17 April 1998, Orlando, Florida USA, Advanced Technical Program, p.52. Published in Proceedings of SPIE, Vol. 3388.
3. "The development of the optically addressed spatial light modulators for dynamical holography applications using deformed helix ferroelectric liquid crystals with large tilt angle", by L.A.Beresnev, A.P.Onokhov, W.Dultz, M.V.Isaev, N.A.Feoktistov, N.L.Ivanova, E.A.Konshina, A.N.Chaika, V.A.Berenberg, T.Weyrauch and W.Haase. Presented to SPIE Meeting, San Diego, 19-24 July 98, USA, session on "Dynamic measurement, control, and correction approaches for severely aberrated large optics". Article is published in SPIE Proceedings, Vol. 3432, pp.151-162.
4. "Preparation and investigation of optical and photoelectric properties of a-Si:C:H/a-C:H thin film structures for optically addressed spatial light modulators", by E.A.Konshina, A.P.Onokhov, N.A.Feoktistov, W.Dultz, L.A. Beresnev and W. Haase. Presented to SPIE Meeting, San Diego, 19-24 July 98, USA, session on "Dynamic measurement, control, and correction approaches for severely aberrated large optics".
5. "Dynamic Correction for Distorsion in Imaging Optical Systems using Liquid Crystal SLMs", by V. A. Berenberg, A. A. Leshchev, M. V. Vasil'ev, V. Yu. Venediktov, A. P. Onokhov, and L. A. Beresnev, Presented to SPIE Meeting, San Diego, 19-24 July 98, USA, session on "Dynamic measurement, control, and correction approaches for severely aberrated large optics", published in Proceedings of SPIE, Vol. 3432, pp. 110-119.
6. "Deformed-helix ferroelectric liquid-crystal spatial light modulator demonstrating high diffraction efficiency and 370 line pairs per millimeter resolution", by David V. Wick, Ty Martinez, Michael V. Wood, James M. Wilkes, Mark T. Gruneisen, Vladimir A. Berenberg, Michael V. Vasil'ev, Arkady P. Onokhov, and Leonid A. Beresnev, submitted to Applied Optics, 1999.

The abstracts of reports are presented to SPIE Conf. , 19-24 July, 1999, Denver CO, USA:

7. "Polarization non-sensitive optical phase modulators using the deformed helix ferroelectric liquid crystals" by L. A. Beresnev, W. Dultz, B. Hils, T. Weyrauch, S. A. Pikin, W. Haase (sections 2.1.2 and 4.1 of this report). Article will be submitted to SPIE Conf., Denver CO.

   and

8. "Cancellation of effects of large phase distorsion on images by dynamical holography using ferroelectric liquid crystal spatial light modulators" by P. P. Banerjee, L. A. Beresnev, and M. A. Vorontsov.

The Patent Application were filed with German Telekom:

9. "Electrooptical phase modulator", by W. Dultz, L. A. Beresnev, W. Haase, and A. P. Onokhov.
10. "Liquid crystal for optical phase modulation", by W. Dultz, L. A. Beresnev, T. Weyrauch. S. A. Pikin,and W. Haase (see sections 2.1.3 and 2.1.4 of this report)

Literature Cited:

1. R.K.Tyson "Principles of Adaptive Optics", Academic, N.Y. 1991;
2. R.Q.Fugate "Laser beacon adaptive optics", Opt. Photon. News, Vol.5, pp.14-19 (June 1994).
3. M.A.Vorontsov, G.W.Carhart, D.V.Pruidze, J.C.Ricklin, and D.G.Voelz "Image quality criteria for an adaptive imaging system based on statistical analysis of the speckle field", J. Opt. Soc. Am. A , Vol.13, No.7, pp.1456-1466 (1996).
4. J.C.Ricklin "Optical technique for simulating severe phase distortion effects in imaging system performance", Optics and Photonics News, Dec.1995, pp.15-16.
5. T.Sonehara, J.Amako "Phase modulated liquid crystal spatial light modulator with VGA resolution", Spatial Light Modulators OSA Topical Spring Meeting, Hyatt Regency Lake Tahoe, Incline Village, Nevada USA, March 1997, Technical Digest, p.120, STuE7-1.
6. 6. N.Mukohzaka, N.Yoshida, H.Toyoda, Yuji Kobayashi, and T.Hara "Diffraction efficiency analysis of a parallel-aligned nematic-liquid-crystal spatial light modulator", Applied Optics, Vol.33, No.14, 2804-2811 (1994).
7. L.M.Blinov and V.G.Chigrinov "Electrooptic effects in Liquid Crystal Materials", Springler Verlag, New York, 1993.
8. R.B.Meyer, L.Liebert, L.Strzelecki and P.Keller "Ferroelectric Liquid Crystals", Journal de Phys.-Lett., Vol.36, p.L69-L71 (1975).
9. N.A.Clark, and S.T.Lagerwall "Submicrosecond bistable electro-optic switching in liquid crystals", Appl.Phys.Lett., Vol.36, 899-901 (1980).
10. S.T.Lagerwall, N.A.Clark, J.Dijon, and J.F.Clerc "Ferroelectric liquid crystals: the development of devices", Ferroelectrics, Vol.94, 3-62 (1989);
11. M.A.Handschy, D.B.Banas, and S.D.Gaalema "Multipurpose spatial light modulator", in: "Spatial Light Modulators and Applications", 1993 Technical Digest Series, Vol.6, OSA, Washington, DC, 1993b, pp.62-65.
12. G.Moddel "Ferroelectric Liquid Crystal Spatial Light Modulators", in: "Spatial Light Modulator Technology", Marcel Dekker,Inc., ed. by U.Efron, New York, Basel, Hong Kong, 286-359 (1994).
13. J.R.Lindle, F.J.Bartoli, S.R.Flom, B.R.Ratna, and R.Shashidhar "Field-Dependent Birefringence of an Electroclinic Liquid Crystal", in: Spatial Light Modulators OSA Topical Spring Meeting, Hyatt Regency Lake Tahoe, Incline Village, Nevada USA, March 1997, Technical Digest, p.151-153, SWB3-1.
14. L.A.Beresnev, V.G.Chigrinov, D.I.Dergachev, M.V.Loseva, N.I.Chernova, E.P.Pozhidayev, B.I.Ostrovskii, A.Z.Rabinovich, A.V.Ivashchenko, V.V.Titov and M.Schadt "Ferroelectric liquid crystal display", Swiss Patent *"Ferroelektrische Flüsigkristallanzeige"*, No.3722/87, Ref.RAN 4701/127-002, September 21, 1987.
15. L.A.Beresnev, L.M.Blinov, and D.I,.Dergachev "Electrooptical response of a thin layer of a ferroelectric liquid crystal with a small pitch and high spontaneous polarization", Ferroelectrics, Vol.85, pp.173-186 (1988).
16. L.A.Beresnev, V.G.Chigrinov, D.I.Dergachev, E.P.Pozhidayev, J.Fünfschilling, and M.Schadt "Deformed helix ferroelectric liquid crystal display: A new electrooptical mode in ferroelectric chiral smectic C liquid crystals", Liquid Crystals, Vol.5, pp.1171-1177 (1989).
17. W.K.Choi, A.B.Davey and W.A.Crossland "Use of Deformed Helix Ferroelectric Liquid Crystals in Fabri Perot Etalons", Ferroelectrics, Vol.181, pp.11-19 (1996).
18. Johannes Eschler, Stefan Dickmann and Dieter A.Mlynski "Fast Adaptive Lens Based on Deformed Helical Ferroelectric Liquid Crystal", Ferroelectrics, Vol.181, pp.21-28 (1996).
19. S. A. Pikin, *Structural Transformations in Liquid Crystals* (Gordon&Breach, New York, 1991)
20. G.Andersson, I.Dahl, L.Komitov, S.T.Lagerwall, K.Skarp, and B.Stebler "Device Physics of Soft Mode (Electroclinic) Effect", J.Appl.Phys., Vol.66, 4983 (1989).
21. L.A.Beresnev, W.Dultz, A.P.Onokhov, S.Hiller and W.Haase "Research, development and performance of FLC devices using soft-mode (electroclinic) effect", 24. Freiburger Arbeitstagung Flüssigcrystalle, 1995, Proceedings, O4.
22. L.A.Beresnev, W.Dultz, Th.Weyrauch and W.Haase "The device for switching of optical images with microsecond response time" Deutsches Patent "Bauelement zum Schalten von optischen mustern in der zeiteinheit von Mikrosekunden" No. 196 31 644.8, filed August 5, 1996.
23. Francois Tournilhac, Jacques Simon, “Structural properties of polyphilic mesogens. Toward longitudinal ferroelectricity”, Ferroelectrics, **114**, 283-287 (1991).

24. F. G. Tournilhac, L. Bosio, J. Simon, L. M. Blinov, and S. V. Jablonsky, "Synthesis of polyphilic compounds. Evidence for ferroelectricity in a non-chiral mesophase", Liquid Crystals, **14**, 405-414 (1993).
25. Hong Liu and Hiroyuki Nohira, "Synthesis of semi-perfluorinated FLCs and the effect of fluorination extent on mesomorphic properties", Mol. Cryst. Liq. Cryst., **302**, 257-252 (1997).
26. M. T. Gruneisen, K. W. Peters and J. M. Wilkes, "Compensated Imaging by Real-Time Holography with Optically Addressed Liquid-Crystal Spatial Light Modulator", Proc. of SPIE, **3143**, pp171-181 (1997).
27. L.A.Beresnev, J.Hossfeld, W.Dultz, A.P.Onokhov and W.Haase, "Demonstration set-up for fast switchable diffraction of lasewr light using the computer controlled diffraction grating based on ferroelectric liquid crystal", Mat. Res. Soc. Proc., Vol. **413**, 363-370 (1996).
28. S. Fukushima and T. Kurokawa, "Real-time hologram construction and reconstruction using a high-resolution spatial light modulator", Appl. Phys. Lett. **58**, pp.787-789 (1991).
29. C. C. Mao, K. M. Johnson, and G. Moddel, "Optical phase conjugation using optically addressed chiral smectic liquid crystal spatial light modulators", Ferroelectrics, **114**, pp.45-53 (1991).
30. "Novel liquid crystal spatial light modulators for adaptive optics and image processing" by A. P. Onokhov, V. A. Berenberg, A. N. Chaika, N. L. Ivanova, M. V. Isaev, N. A. Feoktistov, L. A. Beresnev, and W. Haase, presented to SPIE's 12 Annual Int. Symp. "AeroSense", section "Advances in Optical Information Processing VIII", 13-17 April 1998, Orlando, Florida USA, Advanced Technical Program, p.52. Published in Proceedings of SPIE, Vol. 3388.
31. "Polychromatic correction for aberrations in the lenses of telescopic systems using liquid-crystal optically addressed spatial light modulators", by V. A. Berenberg, M. V. Vasiliev, V. Yu. Venediktov, A. A. Leshchev, L. N. Soms, A. P. Onokhov, L. A. Beresnev, and W. Haase, presented to SPIE's 12 Annual Int. Symp. "AeroSense", section "Advances in Optical Information Processing VIII", 13-17 April 1998, Orlando, Florida USA, Advanced Technical Program, p.52. Published in Proceedings of SPIE, Vol. 3388.
32. "Dynamic Correction for Distorsion in Imaging Optical Systems using Liquid Crystal SLMs", by V. A. Berenberg, A. A. Leshchev, M. V. Vasil'ev, V. Yu. Venediktov, A. P. Onokhov, and L. A. Beresnev, Presented to SPIE Meeting, San Diego, 19-24 July 98, USA, session on "Dynamic measurement, control, and correction approaches for severely aberrated large optics", published in Proceedings of SPIE, Vol. 3432, pp. 110-119.
33. "Deformed-helix ferroelectric liquid-crystal spatial light modulator demonstrating high diffraction efficiency and 370 line pairs per millimeter resolution", by David V. Wick, Ty Martinez, Michael V. Wood, James M. Wilkes, Mark T. Gruneisen, Vladimir A. Berenberg, Michael V. Vasil'ev, Arkady P. Onokhov, and Leonid A. Beresnev, submitted to Applied Optics, 1999.
34. "Cancellation of effects of large phase distorsion on images by dynamical holography using ferroelectric liquid crystal spatial light modulators" P. P. Banerjee, L. A. Beresnev, and M. A. Vorontsov, report abstracts presented to SPIE Conf. , 19-24 July, 1999, Denver CO, USA.

List of Content.

Appendix. Possible positions of the perfluorinated chain in the dimer banana shape molecules formung the liquid crystal for phase modulation.

The presence of the perfluorinated chain 44 is necessary, according to the section 2.1.4, for the preventing the flip-flop effect for chiral dimers, described in Fig.19. The perfluorinated fragment 44 should be in the asymmetric position relative to the tip 6 of the dimer. It can be realized by different ways. The perfluorinated fragment 44 can be introduced instead of the hydrocarbon chain 36, as it is shown in Fig's 21,22, it can be added to this hydrocarbon chain 36 outside of molecule, as it is shown in Fig.34, or close to the central core 2, as it is shown in Fig.35.

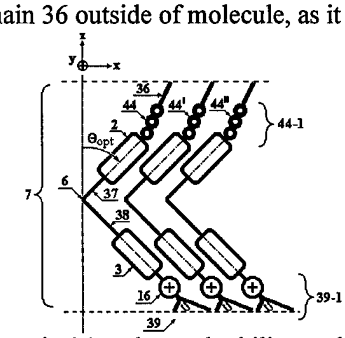

Fig.34. The polyphilic molecules with the perfluorinated chain 44 connected to the aliphatic hydrcarbon tail 36 outside of central core 2 between said core 2 and aliphatic chain 36.

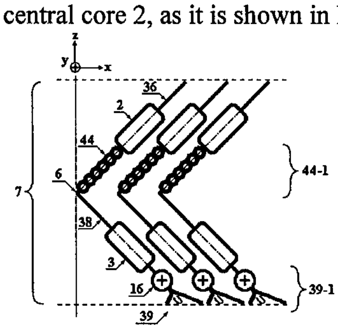

Fig.35. The polyphilic molecules with the perfluorinated chain 44 replacing the aliphatic chain 37 and connected to the aliphatic hydrcarbon chain 38 inside of central cores 2 and 3, close to the core 2 .

The pefluorinated fragment 44 can be inside of dimer in the oposite core from dimer sub-unit, containing the chiral fragment, as it is shown in Fig's 34,35,36, or it can be in the same dimer's sub-unit containing the chiral fragment 39, as it is shown in Fig's 37,38,39. The position of the pefluorinated fragment 44 outside of the central cores, as it is shown in Fig's 21, 22, 34, 38, 39 is more preferable in comparison with the positions inside of central cores, as it is shown in Fig's 35, 36, 37 due to the higher polyphilic asimmetry of the dimers, hence higher degree of the segregation of perfluorinated fragments 44, 44', 44"...

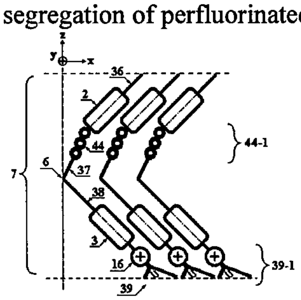

Fig.36. The polyphilic molecules with the perfluorinated chain 44 connected to the aliphatic hydrcarbon tail 37 inside of central cores 2 and 3, close to the core 2.

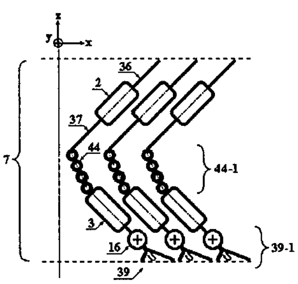

Fig.37. The polyphilic molecules with the perfluorinated chain 44, replacing the aliphatic chain 38 inside of central cores 2 and 3, close to the core 3.

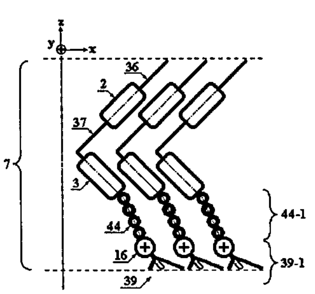

Fig.38. The polyphilic molecules with the perfluorinated chain 44 introduced between central core 3 and transverse dipole moment 16.

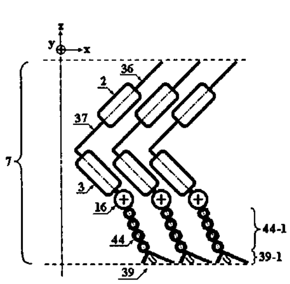

Fig.39. The polyphilic dimer molecules with the perfluorinated chain 44 introduced between transverse dipole moment 16 and chiral fragment 39.

Possibility of two chiral fragments in the banana shape polyphilic dimers.

The value of the spontaneous polarization related with the presence of the chiral fragment 39 and transverse dipolar moment 16 as well as the value of the pitch of helix can be strongly modified by means of introduction of the second chiral fragment 46 to the dimer molecules, Fig's 40, 41. In general this fragment should have another shape and/or another value of the transverse dipolar moment 45. It can be realized using the another molecular fragments 47, 48 and 49 for the design of the second chiral group 46 in the dimer sub-unit with central core 2, compared to the constituent parts 40, 41, and 42, forming the chiral fragment 39 of the opposite dimer's sub-unit 3. In the best case the dipolar moments 16 and 45 in both sub-units will have the same direction, as it is shown in Fig's 21 and 22. Otherwise, in case of the opposite directions the summary dipole moment of the neughbour layers, hence the value of the spontaneous polarization, will be determined by the difference between values 45 and 16 , and in the worse case of the equal values 45 and 16 the spontaneous polarization will be cancelled.

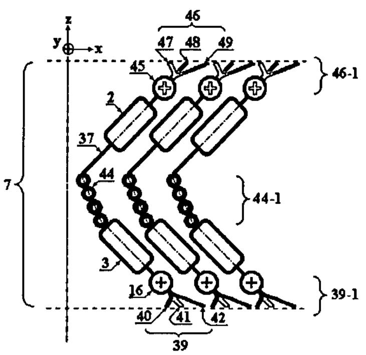

Fig 40. The polyphilic dimer molecules having two chiral fragments 39 and 46 , and two transverse dipole moments 16 and 45. The perfluorinated chain 44 is introduced between central cores 2 and 3 and replaces the aliphatic chain 38.

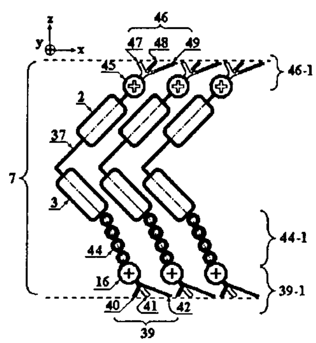

Fig 41. The polyphilic dimer molecules having two chiral fragments 39 and 46 , and two transverse dipole moments 16 and 45. The perfluorinated chain 44 is introduced between central cores 3 and chiral fragment 39.

Ferroelectric and antiferroelectric helical smectic liquid crystals composed from banana shape dimer molecules.

Smectic layers 7, Fig.2, with the described dimer banana shape molecules 1 can form the ferroelectric packing of the neighbour layers as it is shown in Fig.11,12,42 and 45, if the summary dipolar moments of the neighbour layers have the same directions in layers 7, 7-1 and so on. The neughbour smectic layers 7 and 7A can form the antiferroelectric packing, as it is shown in Fig's 13, 43, 44, 46, 47, if the summary dipolar moments of the neighbour layers have the opposite directions.

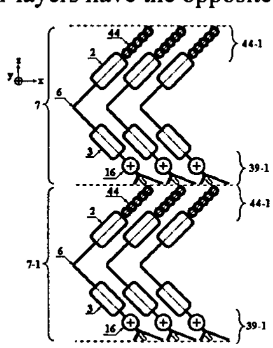

Fig.42. Ferroelectric packing of the neughbour layers 7 and 7-1 with the summarization of the dipole moments 16 of adjaicent layers. The tips 6 of adjaicent layers are directed in the same dirtection.

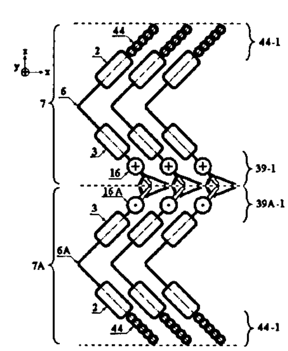

Fig.43. Antiferroelectric packing of the neughbour layers 7 and 7A. The dipole moments in neoughbour layers have opposite directions. The tips 6 and 6A, respectively, have the same directions.

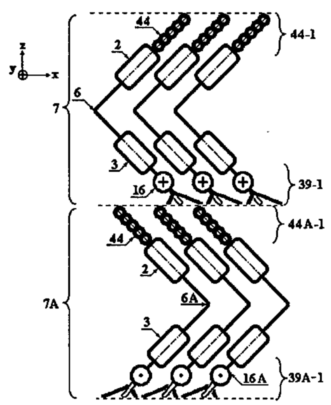

Fig.44 Antiferroelectric packing of the neughbour layers 7 and 7A. The dipole moments in neughbour layers have opposite directions. The tips 6 and 6A, respectively, have also the opposite directions.

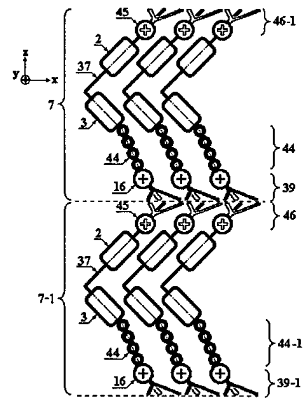

Fig.45. Ferroelectric packing of the neugbour layers 7 and 7-1 for dimer molecules,having two chiral fragments and two transverse dipole moments in accordance with case, shown in Fig.22.

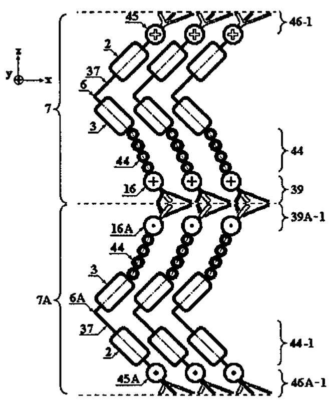

Fig.46. Antiferroelectric packing of the neughbour layers 7 and 7A for dimer banana shape molecules, shown in Fig.22. The summary dipole moments of the neughbour layers have the opposite directions. The tips 6 and 6A in neughbour layers have the same directions.

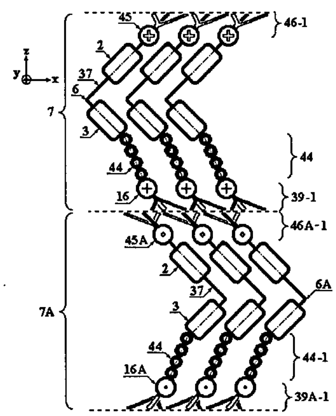

Fig.47. Antiferroelectric packing of the neughbour layers 7 and 7A for dimer banana shape molecules, shown in Fig.22. The summary dipole moments of the neughbour layers have the opposite directions. The tips 6 and 6A in neughbour layers have also the opposite directions.

The difference of the antiferroelectric packing between structures, shown in Fig's 43 and 44, as well as between 46 and 47 is related with the mutual orientations of the tips 6 and 6A in the neughbour layers. In structures, shown in Fig's 43 and 46 the tips 6 and 6A have the same directions, whereas in structures shown in Fig's 44 and 47 the tips 6 and 6A have the opposite directions. The optical properties of all the ferroelectric as well as of the antiferroelectric structures are the same, if the pitch of helix is less than wavelength, and are characterized by refractive index ellipsoid which doesn't change their initial orientation along the helix, or along the normal to smectic layers z. Under influence of the electric field applied along the smectic layers (along the axis y) the increase of the refractive index component $<n_x>$ along the x axis takes place and phase modulation only will take place for the light polarization plane along x axis.